Dawson Voids Water Quality Water Balance modelling

Post-Closure Water Quantity and Quality

PREPARED FOR
AASC

DATE
28 March 2024

REFERENCE
0655820

DOCUMENT DETAILS

DOCUMENT TITLE	Dawson Voids Water Quality Water Balance modelling
DOCUMENT SUBTITLE	Post-Closure Water Quantity and Quality
PROJECT NUMBER	0655820
Date	28 March 2024
Version	01
Author	Nathan Wang
Client name	AASC

DOCUMENT HISTORY

				ERM APPROVAL TO ISSUE		
VERSION	REVISION	AUTHOR	REVIEWED BY	NAME	DATE	COMMENTS
Draft	0	Nathan Wang	Chris Gimber	Chris Gimber	28-02-2024	Draft only- to be updated
Draft	1	Nathan Wang	Chris Gimber	Chris Gimber	28-03-24	Issued to client

SIGNATURE PAGE

Dawson Voids Water Quality Water Balance modelling

Post-Closure Water Quantity and Quality

0655820

[Double click to insert signature]

Nathan Wang
Managing Consultant

[Double click to insert signature]

Chris Gimber
Partner

CONTENTS

LIST OF TABLES

LIST OF FIGURES

ACRONYMS AND ABBREVIATIONS

Acronyms	Description
ACCESS	Australian Community Climate and Earth System Simulator
AHD	Australian Height Datum
ANZECC	Australian and New Zealand Environment and Conservation Council
ASL	Above sea level
AWBM	Australia Water Balance Model
DCN	Dawson Central / North Mine
DEM	Digital Elevation Model
DESI	Department of Environment, Science and Innovation
GIS	Geographic Information System
IPCC	Intergovernmental Panel on Climate Change's
mg/L	milligrams per litre
ML	Mining Lease
QA/QC	Quality Assurance / Quality Control
RCP	Representative Concentration Pathways
RL	Reduced Level
SRES	Special Report on Emission Scenarios
TDS	Total Dissolved Solids
TSF	Tailing Storage Facilities
°C	Degrees Celsius
μS/cm	Micro siemens per centimetres

1. MODEL APPROACH AND ASSUMPTIONS

The Post-Closure Water Quantity and Quality model for the Dawson Mining Complex (Dawson) was developed utilizing Goldsim software version 14.0 (Goldsim, 2021) and its contaminant transport module. Primary components influencing the hydrological equilibrium, inclusive of variables like precipitation, evaporation, and parameters inherent to the Australia Water Balance Model (AWBM), were derived from the 2022 update of the water balance model conducted by KCB. The groundwater flow inputs were simulated using a hydrogeological model, the specifics of which were furnished by KCB (see reference). Additionally, geochemical source terms pertaining to total dissolved solids (TDS) were integrated to proactively assess the water quality within each void.

1.1 CONCEPTUAL MODEL

Figure 1 shows the conceptual model of the water balance during post-closure. The key inflows and outflows are:

- Inflow
  - Precipitation on the water surface
  - Surface runoff from the surrounding catchments
  - Surface runoff and baseflow from the pit shell not inundated by the pit lake
  - Baseflow and seepages from the surrounding catchment and spoils
  - Groundwater inflow
- Outflow
  - Evaporation from the free water surface
  - Groundwater outflow (where relevant)

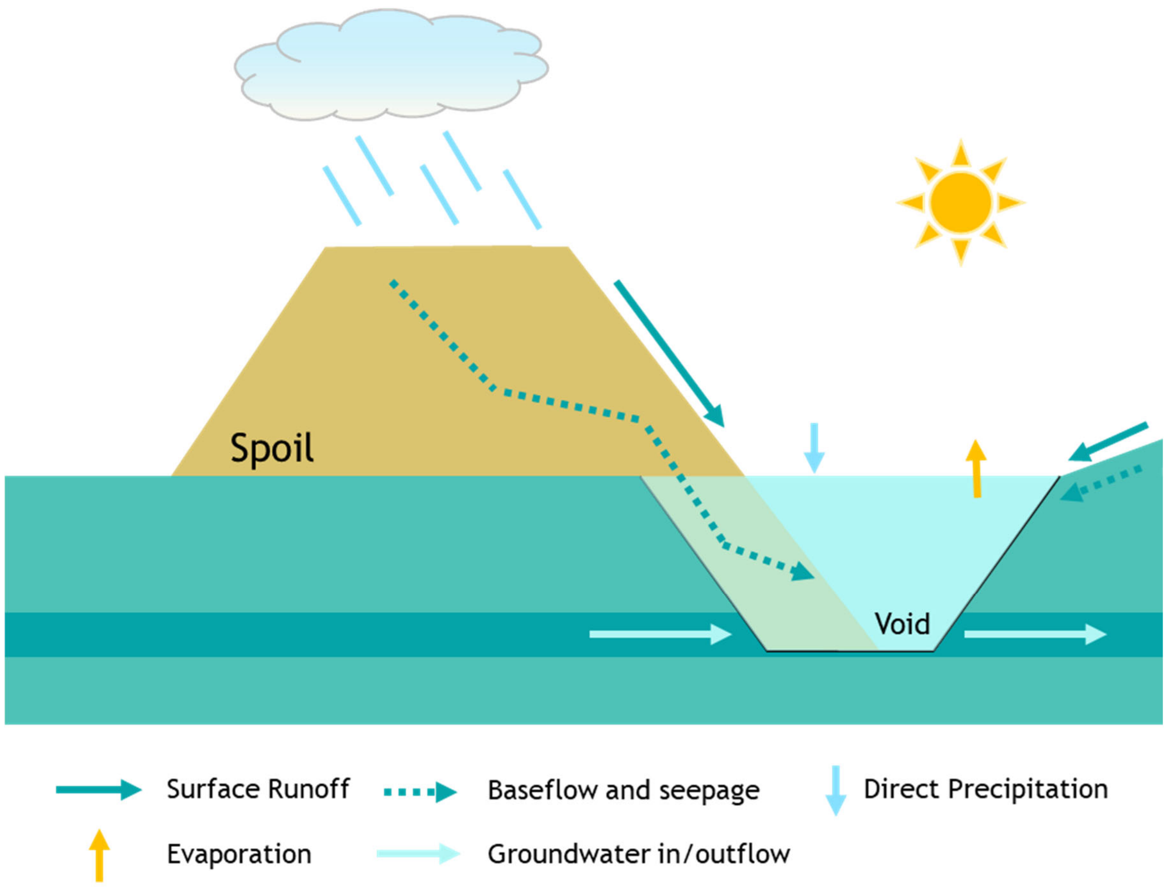

FIGURE 1-1 CONCEPTUAL FLOW DIAGRAM OF DAWSON VOIDS WATER BALANCE AND QUALITY MODEL.

1.2 MODEL SETUP AND ASSUMPTIONS

In the water balance model, water flow and storage change were calculated for each void based on the following equation:

$$S_t = S_{t-1} + RO_s + RO_b + GW_i + P - E - GW_o$$

Where:

S_t=Water volume of the void at time step t;

RO_s = inflow of surface runoff;

RO_b = inflow of baseflow, including seepage from surrounding spoils;

GW_i = groundwater inflow;

P= direct precipitation;

E= evaporation;

GW_o= Groundwater outflow.

The computation of direct precipitation and evaporation from the water surface was predicated on the temporal variation in the surface water area. Within the modeling framework principal inflows encompassing surface runoff and baseflow were determined utilizing the AWBM. The model employed three surface stores to emulate distinct runoff areas within the catchment. Saturation overland flow was conceptualized as the residual rainfall surplus subsequent to the replenishment of the catchment's surface storage capacity. The extent of rainfall abstraction was contingent upon the antecedent moisture conditions of the catchment. The model executed the water balance assessment for each distinct area on a daily basis. At each time increment, rainfall contributed to each of the three surface stores, while evaporation was subtracted from each store. In instances where the stored water exceeded the designated capacity, surplus water translated into runoff. A portion of the excess runoff could potentially recharge the baseflow store, contingent upon the presence of a baseflow component. A schematic representation of the AWBM model is depicted in Figure 2. The parameters utilized in the AWBM, as detailed in Table 1, were derived from the updated Dawson water balance model of 2022.

The following assumptions were relevant to the assessment, and justification is provided below:

1. Each void was treated as an isolated entity in the water balance model, with interactions assessed through the groundwater model inputs to the water balance model.

2. Two land types were adopted for the hydrology model based on the catchment response - spoil and pit wall.

3. The water representation within each void encompasses both the unconfined water within the void and the pore water within the waste rock positioned in the pit shell. The water level was determined by considering the storage curve of each pit shell, accounting for both the unconfined water and pore water. However, the computation of evaporation exclusively considered the surface area of the unconfined water.

4. The pore water level in the waste rock within each pit follows the movement of the free water level in each void, maintaining a consistent relationship between them.

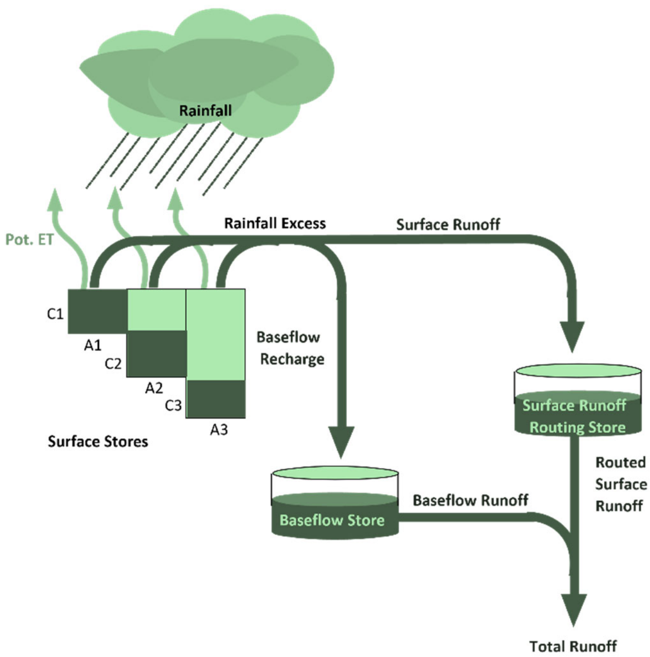

.

FIGURE 1-2 SCHEMATIC DIAGRAM OF AWBM

In the computation of water quality, the mass load, derived from the integration of water quality source terms and flow rates, was incorporated into each water stream. The intricate calculations pertaining to mass loading and its release into the water column were entirely adopted from the 2022 update of the water balance model. (Engeny, 2023).

TABLE 1-1 AWBM PARAMETERS

Parameter	Unit	Mining Pit	Rehabilitated	Spoil
C1	mm	12	30	15
C2	mm	38	80	55
C3	mm	0	200	120
A1	-	0.1	0.134	0.134
A2	-	0.9	0.433	0.433
A3	-	0	0.433	0.433
BFI	-	0	0.5	0.5
Kb	-	0	0.95	0.95
Ks	-	0	0	0

1.3 MODEL SCENARIOS

Model scenarios were conducted with different catchment sizes derived from the final landform and climate data:

Scenario 1: Flow from original Catchment only.

Scenario 2: Flow from original Catchment, with baseflow from spoils nearby (e.g. pit shell area).

Scenario 3: Flow from original Catchment, with baseflow from spoils nearby (e.g. pit shell area) under climate change condition.

1.4 MODEL INPUTS

1.4.1 WATER BALANCE MODEL

The description of water balance inputs including catchment size, geometric information of voids, groundwater flow, along with climate data were summarized in Table 1-2 The coefficients used in AWBM model adopted from the 2022 water balance model were listed in Table 1-2.

TABLE 1-2 WATER BALANCE INPUTS

Input	details	source
Precipitation and evaporation	Historic data covers the period of January 1889 to January 2023 (134 years).	SILO database facility hosted by the Queensland Department of Environment and Science (DES).
Groundwater flow	Timeseries of in/outflow	predicted by a hydrogeologic model and provided by KCB
Geometric information	Storage curve of eight voids, catchment size	Derived from the digital elevation model (DEM) of the final landform

1.4.1.1 CLIMATE INPUT

Inputs for precipitation and evaporation in the Dawson north, center, and south regions were compiled based on long-term historical rainfall and Morton evaporation time-series obtained from the SILO Data Drill service. The SILO Data Drill service extracts gridded climate data interpolated from point observations hosted by the Bureau of Meteorology (BoM). A dataset spanning 134 years, from 1889 to 2023, was utilized in the Monte Carlo model run, incorporating repeated and shifted historical data. The catchment's evaporation was determined by applying a constant ratio of 0.95 to the daily lake evaporation time series. The monthly averages of precipitation and lake evaporation are presented in Table 1-3.

TABLE 1-3 MONTHLY AVERAGE OF PRECIPITATION AND LAKE EVAPORATION APPLIED TO THE DAWSON SITE.

Month	Precipitation			Lake Evaporation		
	North	Center	South	North	Center	South
	mm	mm	mm	mm	mm	mm
Jan	98	96	100	200	200	200
Feb	91	86	91	167	167	167
Mar	68	63	62	163	163	163
Apr	38	36	36	126	125	124
May	33	32	34	93	93	92
Jun	34	34	37	72	71	70
Jul	29	28	30	81	80	79
Aug	21	21	23	108	108	107
Sep	27	27	29	141	140	140
Oct	53	53	55	178	177	176
Nov	67	69	71	192	191	191
Dec	94	88	90	206	206	206
Annual	652	635	657	1728	1722	1713

1.4.1.2 CLIMATE CHANGE SCENARIOS

In the context of the Intergovernmental Panel on Climate Change's (IPCC Fifth Assessment Report AR5), novel Representative Concentration Pathways (RCPs) were introduced to supersede the preceding emission scenarios outlined in the Special Report on Emission Scenarios (SRES)(IPCC, 2013). Diverging from the SRES, the four endorsed RCPs delineate trajectories of greenhouse gas concentrations, as opposed to emissions trajectories. These scenarios, namely RCP2.6, RCP4.5, RCP6, and RCP8.5, corresponding to radiative target forcing levels of +2.6, +4.5, +6.0, and +8.5 W/m^2, respectively, derive their nomenclature from the radiative forcing target for the year 2100. This target is predicated on the forcing exerted by greenhouse gases and other agents, relative to pre-industrial levels (Van et. al., 2011). Figure 3 depicts the concentrations of all forcing agents, expressed in parts per million (ppm) of CO2-equivalence, across the four RCP scenarios.

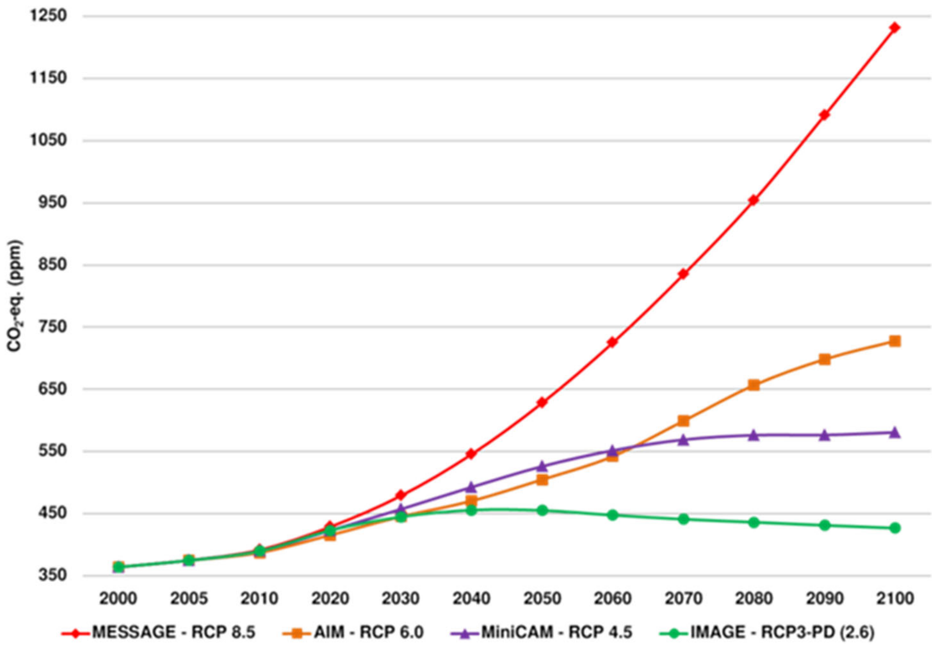

FIGURE 1-3 ALL FORCING AGENTS' ATMOSPHERIC CO2-EQUIVALENT CONCENTRATIONS ACCORDING TO FOUR RCP SCENARIOS.

The Queensland Future Climate Dashboard presented downscaled climate data corresponding to two climate change scenarios, namely RCP8.5 and RCP4.5. Each scenario entailed the provision of 12 model outcomes pertaining to alterations in precipitation and evaporation within the central Queensland region. Within this array of models, the predictions derived from the Australian Community Climate and Earth System Simulator (ACCESS) model, specifically ACCESS1-3 under the RCP 8.5 scenario, were employed in this investigation to assess the impact of climate change on the Dawson void. The percentage shifts in precipitation and evaporation from the year 2020 to 2100 are delineated in Table 1-4 and Table 1-5. These percentage alterations were subsequently applied to the historical climate data inputs within the specified scenario.

TABLE 1-4 CHANGE OF PRECIPITATION PREDICTED BY ACCESS 1-3 MODEL UNDER RCP8.5 SCENARIO FROM 2020 TO 2100.

Month	2020-2039	2040-2059	2060-2079	2080-2099
	% change	% change	% change	% change
Jan	2.7	-4.5	9	15
Feb	2.7	-4.5	9	15
Mar	-9.1	-15	-31	-10
Apr	-9.1	-15	-31	-10
May	-9.1	-15	-31	-10
Jun	1.2	16	-33	-23
Jul	1.2	16	-33	-23

Month	2020-2039	2040-2059	2060-2079	2080-2099
	% change	% change	% change	% change
Aug	1.2	16	-33	-23
Sep	40	-5.6	-10	-33
Oct	40	-5.6	-10	-33
Nov	40	-5.6	-10	-33
Dec	2.7	-4.5	9	15

TABLE 1-5 CHANGE OF EVAPORATION PREDICTED BY ACCESS 1-3 MODEL UNDER RCP8.5 SCENARIO FROM 2020 TO 2100.

Month	2020-2039	2040-2059	2060-2079	2080-2099
	% change	% change	% change	% change
Jan	13	26	28	34
Feb	13	26	28	34
Mar	12	22	36	39
Apr	12	22	36	39
May	12	22	36	39
Jun	11	17	36	40
Jul	11	17	36	40
Aug	11	17	36	40
Sep	3.6	20	32	43
Oct	3.6	20	32	43
Nov	3.6	20	32	43
Dec	13	26	28	34

1.4.1.3 GROUNDWATER FLOW

The associations between water level and groundwater flow rates for each pit shell were provided by KCB and are visually depicted in Appendix B. According to the data, the overarching trend suggests a rise in groundwater inflow as water levels decrease, with the exception of pits in the South mining area. Significantly, Pit 25 and Pit 28 exhibit a projected increase in groundwater inflow concurrent with the elevation of water levels.

1.4.1.4 CATCHMENT SIZE AND STORAGE CURVE

The catchment size, area of each void, elevation of bottom and crest of each void were all delineated and derived from the final landform DEM file received. The summarized information for each void are listed in Table 1-6.

Since the voids are generally surrounded by backfill of the mining shell, base flow from the waste rock placed in the mining pit was assumed to report the final void even the surface landscape of these area is not part of the catchment of the void for scenarios 2 and 3. The extra spoil size of each void was derived from the final landscape surface and prime surface after mining, and listed in Table 1-6.

TABLE 1-6 GEOMETRIC INPUTS OF EACH VOID AND CORESPONDING CATCHMENT

Void name	Catchment size	Extra Spoil size	Max surface area	Max depth
	ha	ha	ha	m
Northern Pit	282	558	344	221
Pit 2	402	371	242	163
Pit3-12	1307	823	634	208
Pit 13	581	370	188	121
Pit 19	814	1225	275	157
Pit 24	120	351	160	68
Pit 25	184	170	162	88
Pit 28	170	600	152	94

1.4.1.5 STORAGE CURVE

The water area-depth curves for the voids were derived using the DEM file representing the final landform. These curves were employed to calculate the free water surface in the model for evaluating evaporation loss. However, the calculation of the void's water level utilized a distinct storage curve. Since most voids are situated on partially filled mining pits, the water level is influenced by the high porosity of the waste rock surrounding the final void. In brief, the assumption was made that the pit would receive all the inflow, and the surface of the free water in the void would ascend in tandem with the water table in the waste rock. In this study, the storage curve considered both the free water column and the pore water in the waste rock within the pit shell. A uniform porosity of 0.4 was assumed and applied to all waste rock in the pit. The storage curves for each void, representing the void alone and the void with additional pore water, have been graphically presented for each void in Appendix A.

1.4.2 WATER QUALITY MODEL

Table 8 consolidates the constant TDS values allocated to runoff from individual sub-catchments, along with values for precipitation and groundwater inflow. The entirety of this data is derived from the 2022 water balance model update conducted by KCB, which is based on a calibrated operational site water balance model.

TABLE 1-7 WATER QUALITY INPUTS

Water type	TDS (mg/L)
Land use Runoff water quality	
Mining Pit	6000
Spoil	6000
Rehabilitated spoil	4000
Other water	
Precipitation	30
Groundwater	8000

2. MODEL RESULTS

2.1 WATER LEVEL

The model outcomes indicate that the water levels in all voids will stabilize after varying durations under the different scenarios assessed. The projected minimum, median, and maximum equilibrium water levels for three scenarios have been documented in Table 2-1. Additionally, the minimum freeboard required to prevent overflow, listed in Table 2-2 for three scenarios, and the estimated time needed to attain equilibrium water levels, presented in Table 11. The changes in water levels for each void post-mining are illustrated in Appendix C.

As per the model results, there is no chance of future overflow in these voids based on the current model configuration. In general, water levels are low for all the voids, especially if only the original catchment size were considered. The minimum predicted freeboard is 32 meters in Pit 24, while the North pit is anticipated to have the largest freeboard, exceeding 100 meters in all three scenarios. Under the climate change scenario, an elevated evaporation rate is expected to expedite the attainment of water level equilibrium for most voids, excluding Pit 2, Pit 3-12, and Pit 28, as these voids possess smaller surface area/volume ratios.

TABLE 2-1 MINIMUM, MEDIAN AND MAXIMUM EQUILIBRIUM WATER LEVEL PREDICTED FOR EACH VOID.

Mining Area	Void ID	Equilibrium Level (m AHD)								
		Scenario 1			Scenario 2			Scenario 3		
		Min	Med	Max	Min	Med	Max	Min	Med	Max
North	**North Pit**	7	10	15	17	21	27	0	2	7
Center	**Pit 2**	71	72	75	72	73	76	50	51	55
	Pit 3-12	52	53	56	53	54	57	20	22	25
	Pit 13	75	77	85	81	83	92	59	61	70
	Pit 19	66	68	73	85	87	92	49	52	59
	Pit 24	89	90	94	92	93	99	82	84	89
South	**Pit 25**	71	73	76	76	78	81	61	63	67
	Pit 28	78	79	80	79	80	83	72	75	77

TABLE 2-2 MINIMUM FREEBOARD PREDICTED FOR EACH VOID.

Mining Area	Void ID	Min Freeboard to Surface Overflow RL (m)		
		Scenario 1	Scenario 2	Scenario 3
North	North Pit	121	109	129
Center	Pit 2	51	50	71
	Pit 3-12	39	38	70
	Pit 13	51	44	66
	Pit 19	62	43	76
	Pit 24	37	32	42
South	Pit 25	59	54	68
	Pit 28	50	47	53

TABLE 2-3 ESTIMATED TIME TO REACH WATER LEVEL EQUILLIBRIUM FOR EACH VOID.

Mining Area	Void ID	Estimated Time to Reach Equilibrium (years.)		
		Scenario 1	Scenario 2	Scenario 3
North	North Pit	120	240	80
Center	Pit 2	240	200	280
	Pit 3-12	300	240	320
	Pit 13	250	280	60
	Pit 19	450	450	150
	Pit 24	100	100	80
South	Pit 25	280	320	100
	Pit 28	320	120	300

2.2 WATER QUALITY

The water quality is anticipated to exhibit a sustained upward trend in each void. This trend is attributed to the concentrating effect induced by the high evaporation rate. The projected TDS concentrations for each void after 100 years are presented in Table 2-4. Generally, a higher TDS corresponds to a greater surface area/volume ratio of the void. Concentration of TDS predicted in Scenario 3 are higher than other two scenarios because climate change condition has the highest evaporation rate. Concentration predicted by Scenarios 1 and 2 are similar. The changes in TDS for each void are graphically represented in the plot found in Appendix D.

The water quality computation employed in this study relies on straightforward assumptions, including a fully mixed water column and conservative mass loading. Nevertheless, the TDS of the water does not indefinitely increase; it precipitates out as a salt when it reaches the saturation limit. Based on the ionic composition this is not expected to occur for any salt species until at least 100,000 mg/l, and widespread precipitation is not expected until concentrations approach mid 200,000 mg/l. Furthermore, the simplistic assumption of a fully mixed water body is not applicable in these deep voids. Stratification is expected to occur in the water column, and a concentration gradient will exist between the free water body and the pore water of the spoil in the pit shell. To accurately predict water quality at various locations within each void, a more sophisticated model must be employed.

TABLE 2-4 PROJECTED TDS CONCENTRATIONS FOR EACH VOID AFTER 100 YEARS

Mining Area	Void ID	TDS after 100 years (mg/L)		
		Scenario 1	Scenario 2	Scenario 3
North	**North Pit**	18,000	17,000	24,000
Center	**Pit 2**	12,000	12,000	16,000
	Pit 3-12	11,000	11,000	14,000
	Pit 13	15,000	15,000	22,000
	Pit 19	12,000	12,000	16,000
	Pit 24	30,000	29,000	48,000
South	**Pit 25**	19,000	18,000	32,000
	Pit 28	9,000	10,000	12,000

3. SUMMARY

Key findings of this study include:

1. No overflow is anticipated in any of the voids across all scenarios, with the minimum predicted freeboard consistently exceeding 30 meters.

2. Water levels projected in Scenario 2 marginally surpass those in Scenario 1, attributed to the higher inflow rate. The predicted water quality exhibits similarities between these two scenarios.

3. Under climate change conditions, voids were projected to have the lowest water levels and the highest concentrations of TDS, due to a high evaporation/precipitation ratio.

4. The stabilization of water levels is forecasted to take 100-450 years under historical climate conditions. For most voids, the time needed for equilibrium is expected to decrease under climate change conditions due to a heightened evaporation rate. However, Pit 2, Pit 3-12, and Pit 28 are anticipated to require similar or longer periods for water level stabilization under climate change conditions, owing to a lower surface area/volume ratio.

5. The concentration of TDS is predicted to continuously rise in all voids based on current assumptions. Nonetheless, a more intricate model will be necessary to accurately predict changes in water quality across all voids.

6. The diverse predicted TDS concentrations in each void are primarily contingent upon the ratio of base flow (groundwater inflow) to total inflow and the surface area/volume ratio specific to each void.

Reference:

Engeny. 2023. *Anglo American Steelmaking Coal-water balance model 2022 update*, Dawson Mining complex 2023.

GoldSim Technology Group (2021), GoldSim (Version 14.0), https://www.goldsim.com, October 2021.

IPCC. 2013. Climate Change 2013: The Physical Science Basis. Contribution of Working Group I to the Fifth Assessment Report of the Intergovernmental Panel on Climate Change. Stocker, T.F., D. Qin, G.-K. Plattner, M. Tignor, S.K. Allen, J. Boschung, A. Nauels, Y. Xia, V. Bex and P.M. Midgley (eds.). Cambridge University Press. Cambridge, United Kingdom and New York, NY, USA.

Van Vuuren, D.P., Edmonds, J., Kainuma, M., Raihi, K., Thomson, A., Hibbard, K. Hurtt, G.C., Kram, T. Krey, V., Lamarque, J.F., et al. 2011. The representative concentration pathways: an overview. Climatic Change. Vol. 109.

ERM

APPENDIX A STORAGE CURVE

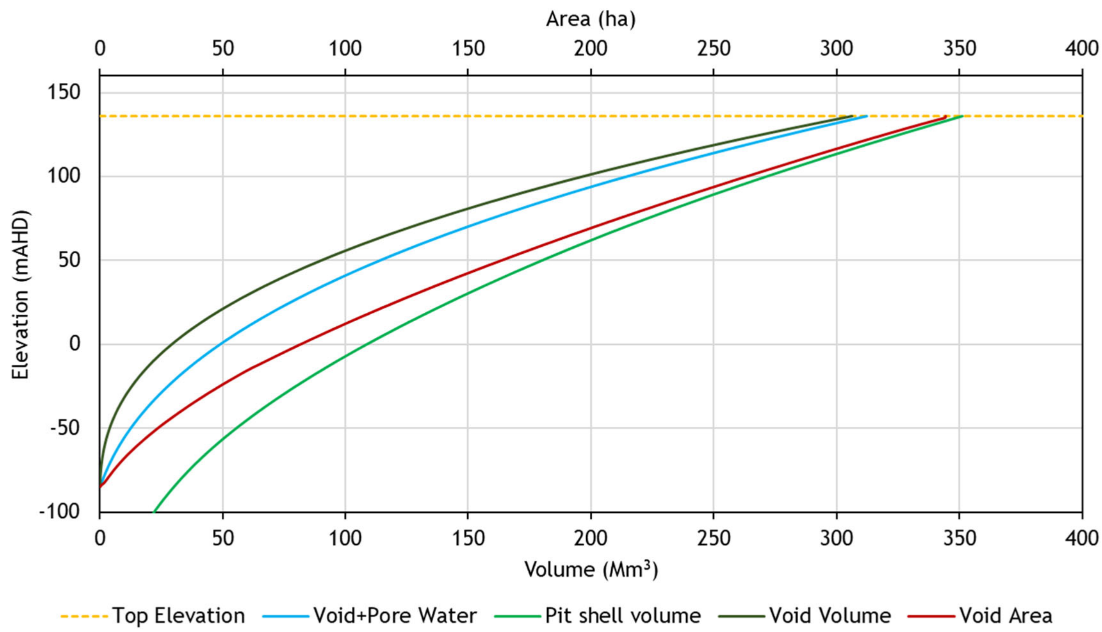

FIGURE A1: STORAGE CURVE OF NORTH PIT SHELL AND VOID, WITH AN ASSUMPTION OF POROSITY 0.4 FOR WASTE ROCK IN PIT.

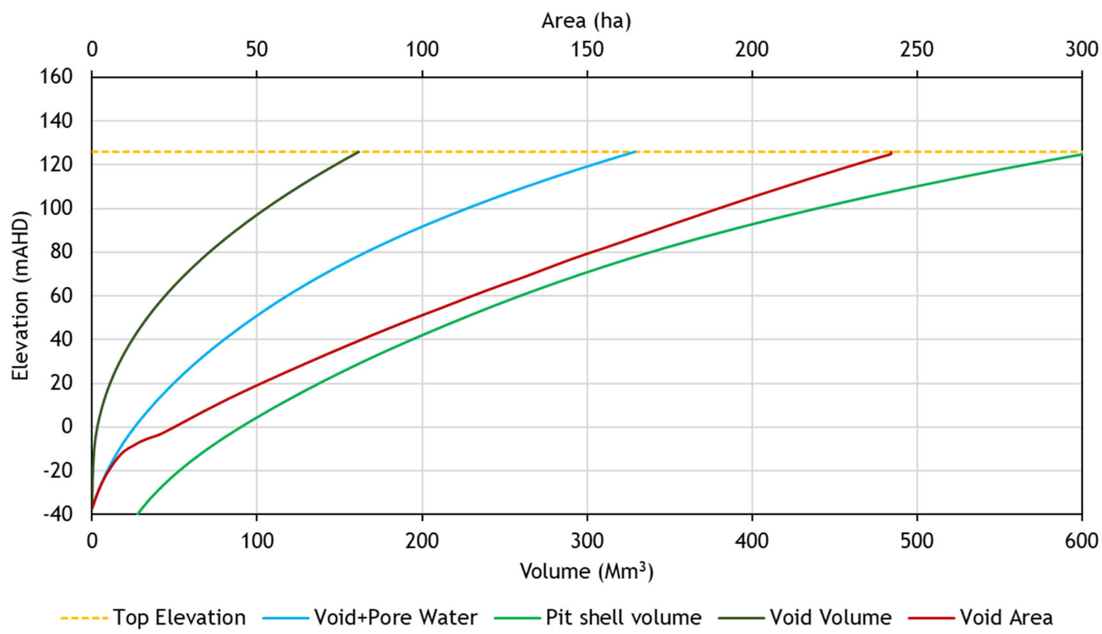

FIGURE A2: STORAGE CURVE OF PIT 2 SHELL AND VOID, WITH AN ASSUMPTION OF POROSITY 0.4 FOR WASTE ROCK IN PIT.

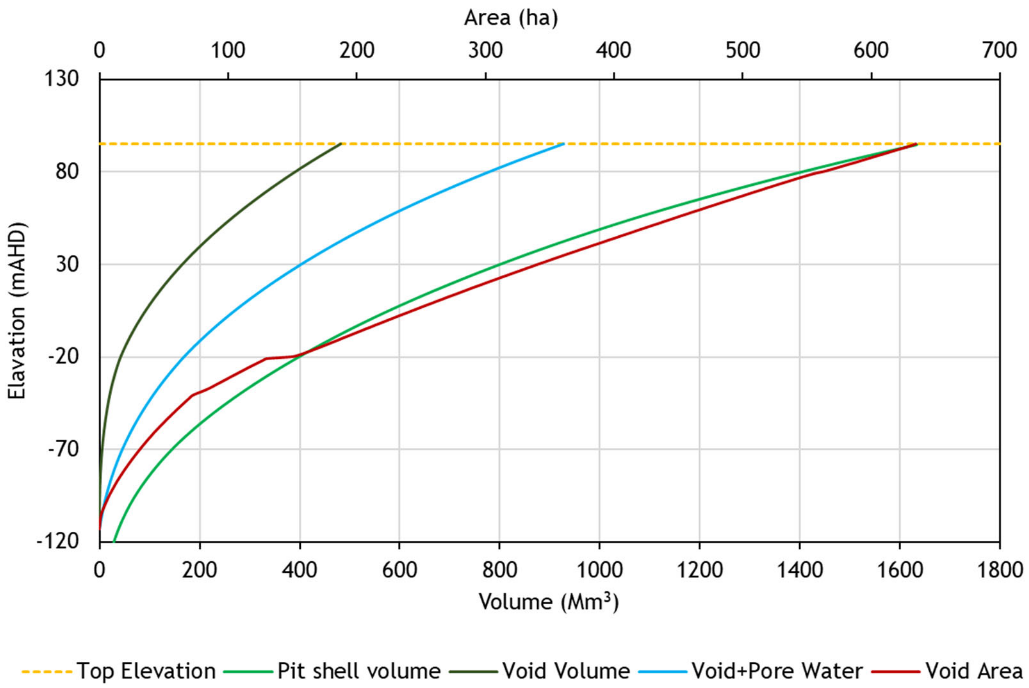

FIGURE A3: STORAGE CURVE OF PIT 3-12 SHELL AND VOID, WITH AN ASSUMPTION OF POROSITY 0.4 FOR WASTE ROCK IN PIT.

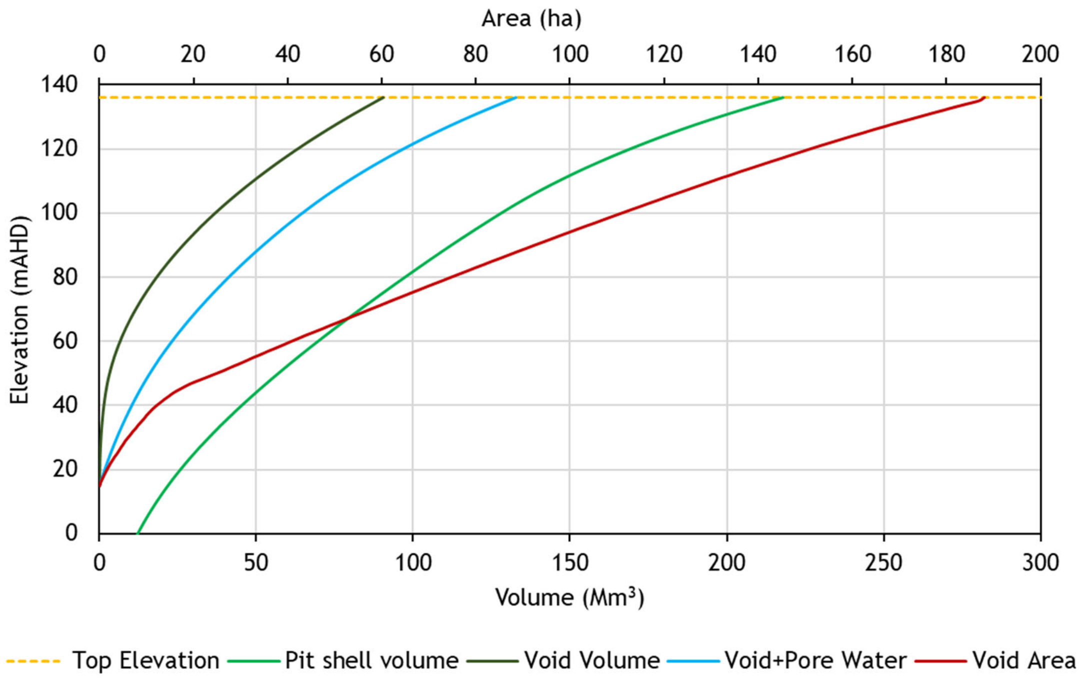

FIGURE A4: STORAGE CURVE OF PIT 13 SHELL AND VOID, WITH AN ASSUMPTION OF POROSITY 0.4 FOR WASTE ROCK IN PIT.

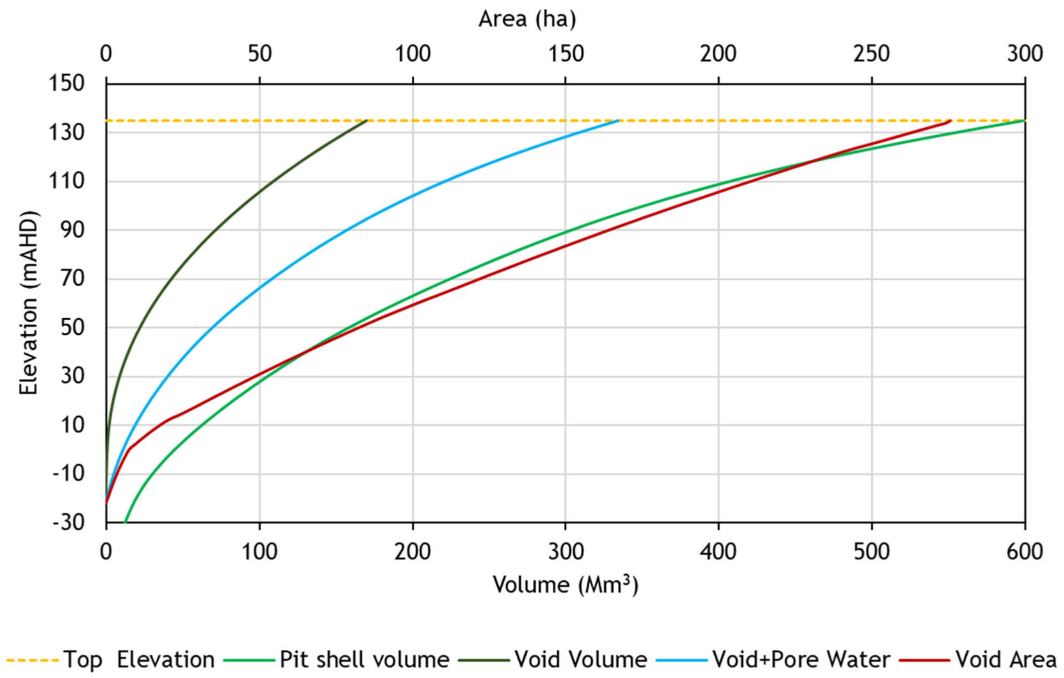

FIGURE A5: STORAGE CURVE OF PIT 19 SHELL AND VOID, WITH AN ASSUMPTION OF POROSITY 0.4 FOR WASTE ROCK IN PIT.

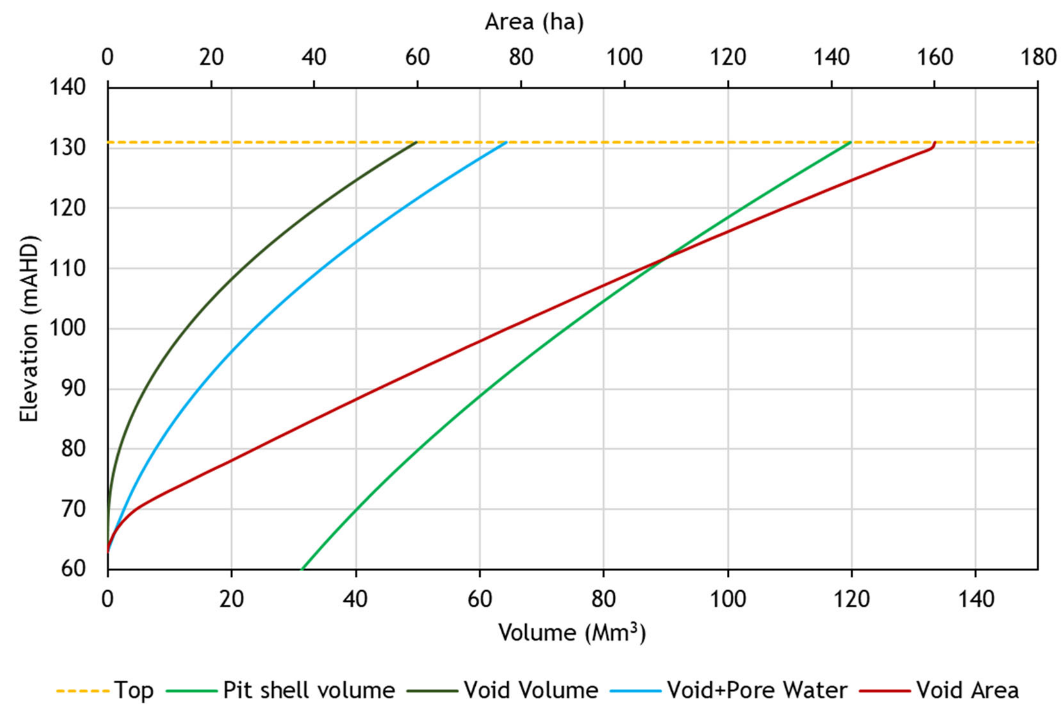

FIGURE A6: STORAGE CURVE OF PIT 24 SHELL AND VOID, WITH AN ASSUMPTION OF POROSITY 0.4 FOR WASTE ROCK IN PIT.

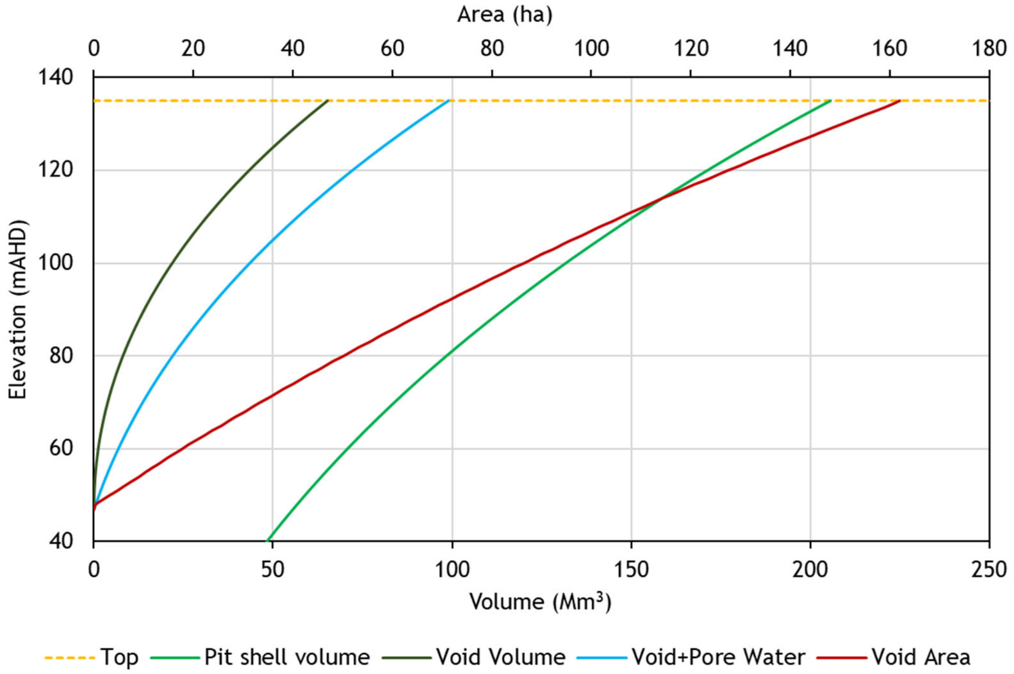

FIGURE A7: STORAGE CURVE OF PIT 25 SHELL AND VOID, WITH AN ASSUMPTION OF POROSITY 0.4 FOR WASTE ROCK IN PIT.

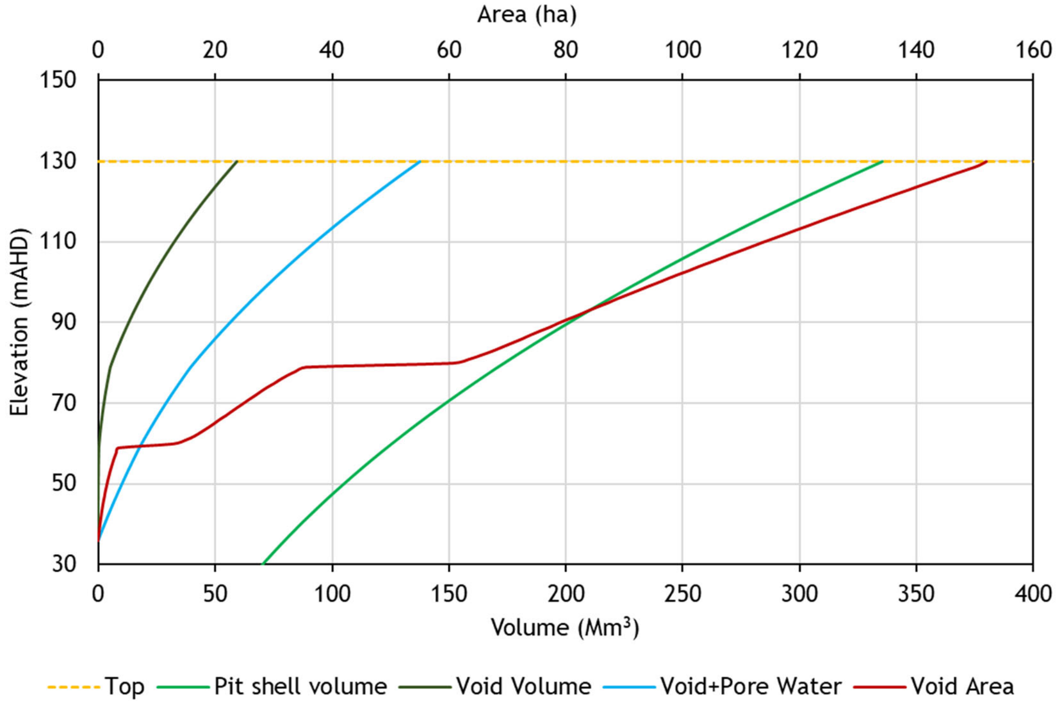

FIGURE A8: STORAGE CURVE OF PIT 28 SHELL AND VOID, WITH AN ASSUMPTION OF POROSITY 0.4 FOR WASTE ROCK IN PIT.

APPENDIX B GROUNDWATER INFLOW

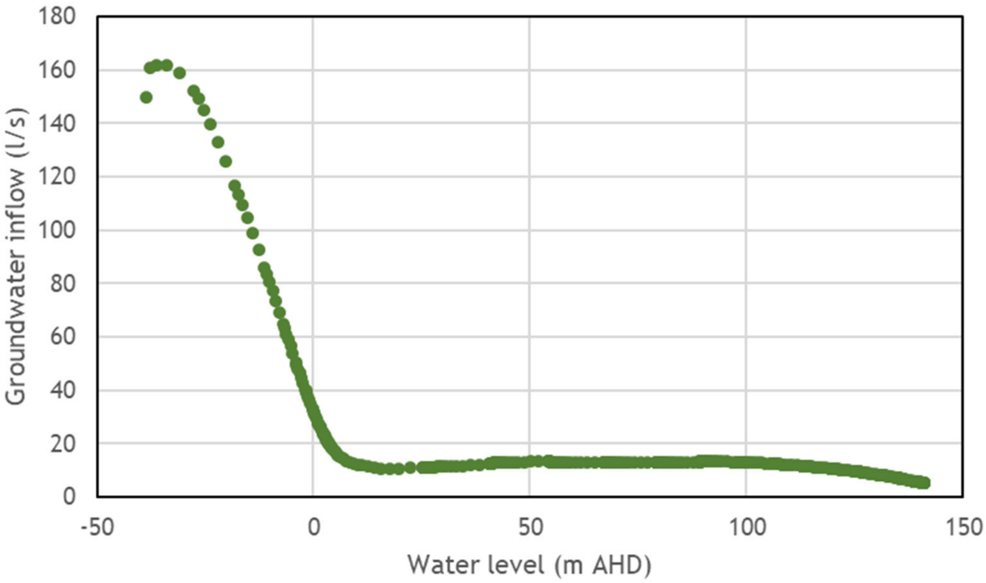

FIGURE B1: WATER LEVEL – GROUNDWATER RELATIONSHIP OF NORTH PIT SHELL.

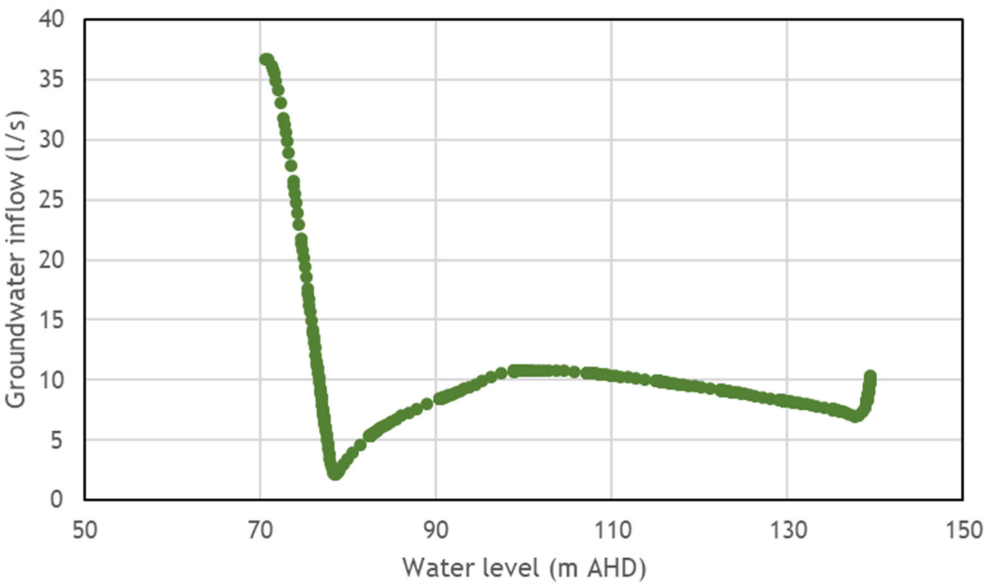

FIGURE B2: WATER LEVEL – GROUNDWATER RELATIONSHIP OF PIT 2 SHELL.

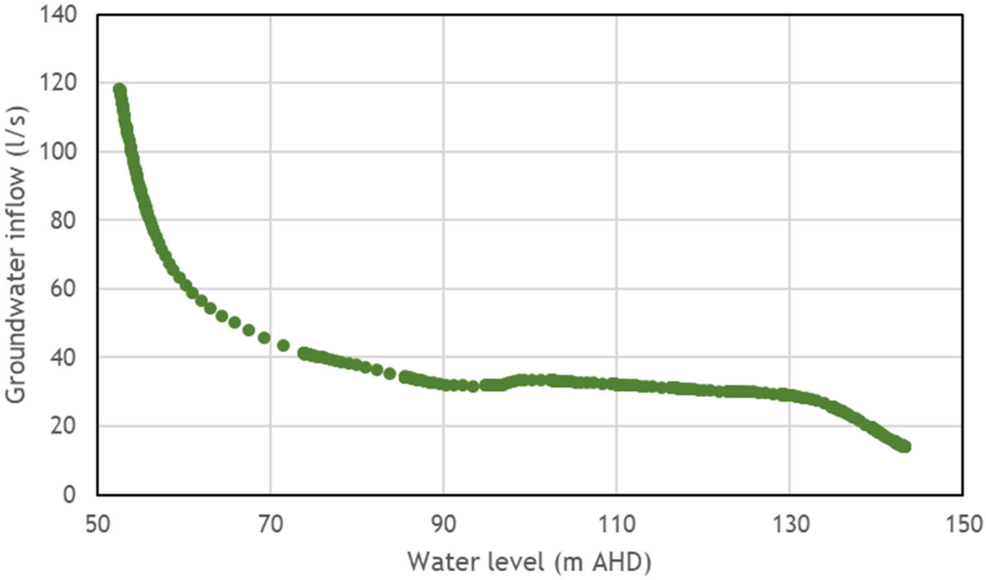

FIGURE B3: WATER LEVEL – GROUNDWATER RELATIONSHIP OF PIT 3-12 SHELL.

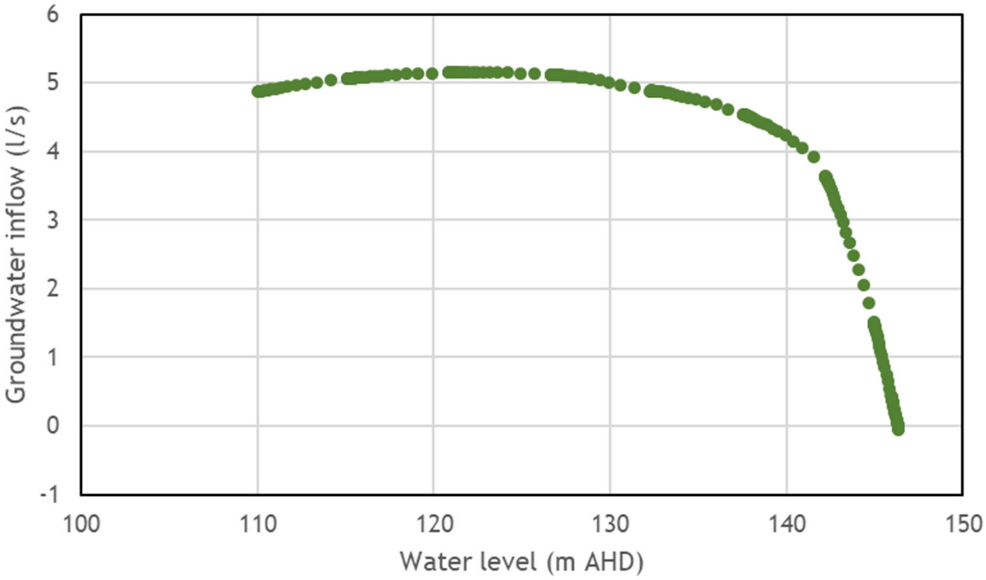

FIGURE B4: WATER LEVEL – GROUNDWATER RELATIONSHIP OF PIT 13 SHELL.

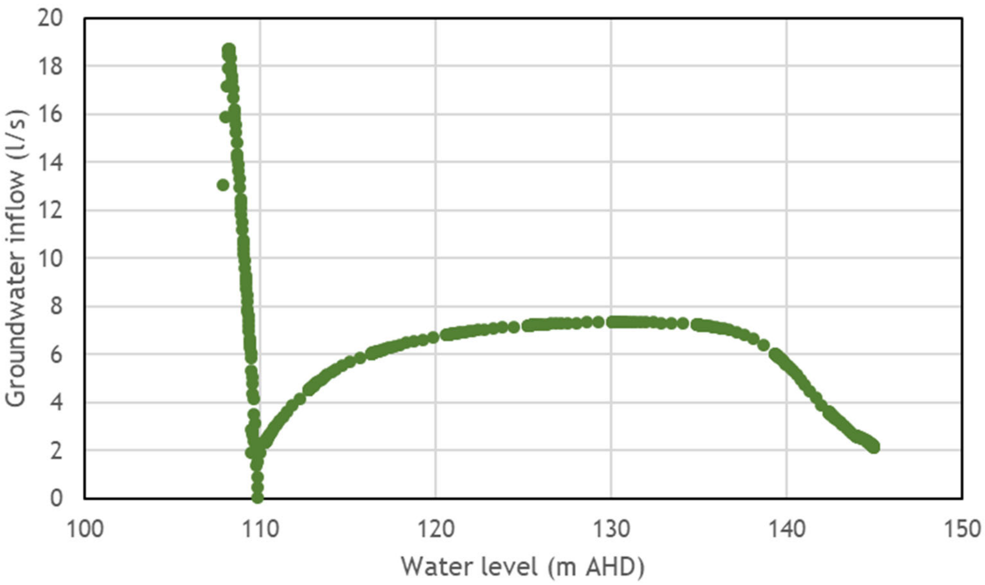

FIGURE B5: WATER LEVEL – GROUNDWATER RELATIONSHIP OF PIT 19 SHELL.

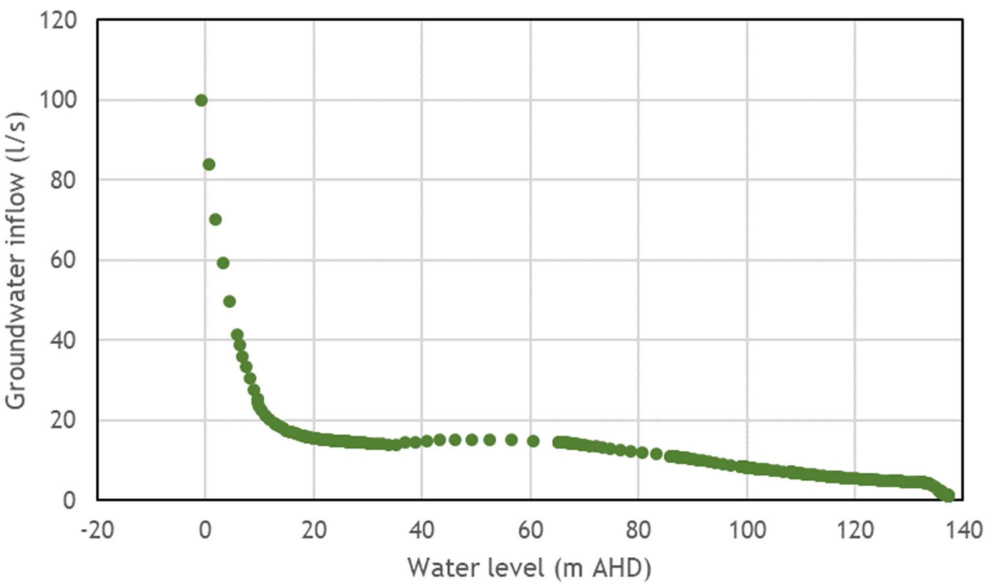

FIGURE B6: WATER LEVEL – GROUNDWATER RELATIONSHIP OF PIT 24 SHELL.

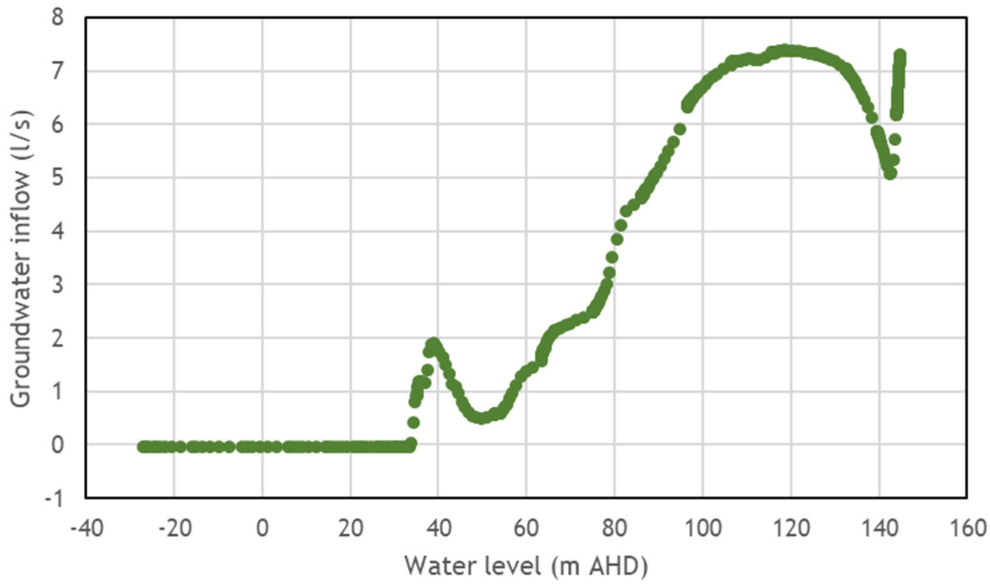

FIGURE B7: WATER LEVEL – GROUNDWATER RELATIONSHIP OF PIT 25 SHELL.

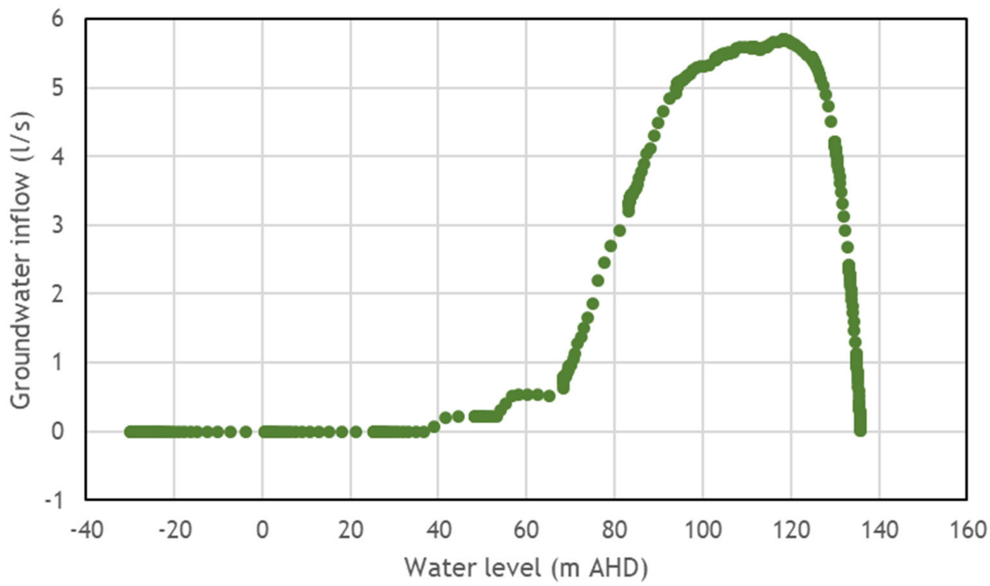

FIGURE B8: WATER LEVEL – GROUNDWATER RELATIONSHIP OF PIT 28 SHELL.

APPENDIX C WATER LEVEL RESULTS

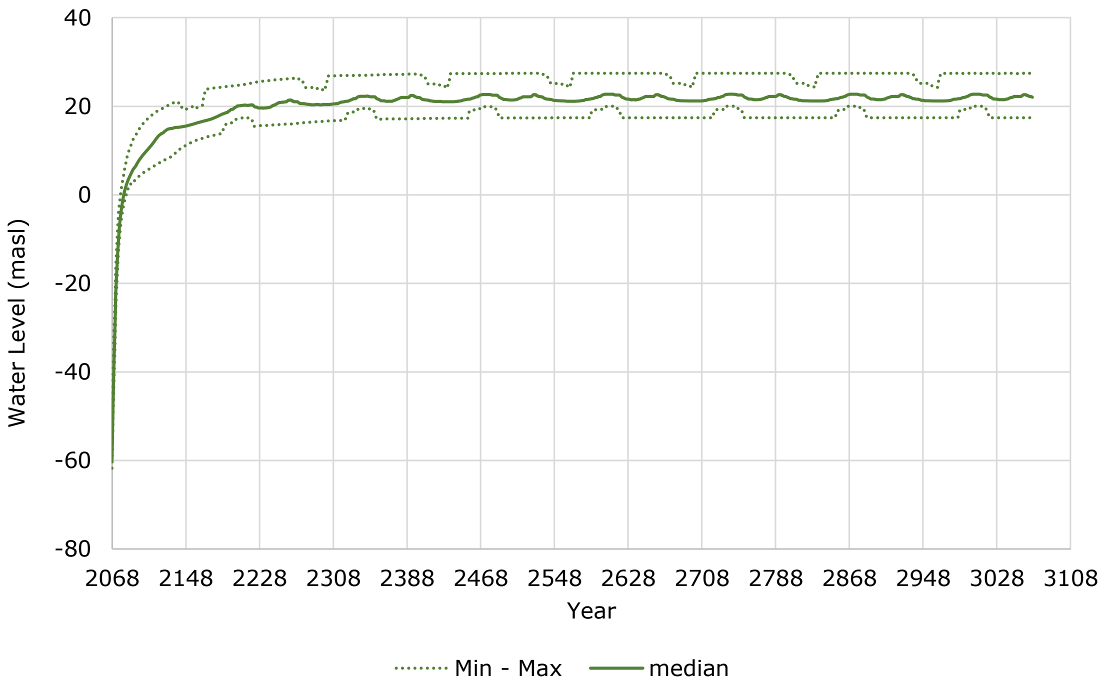

FIGURE C 1.1: PREDICTED WATER LEVEL FOR NORTH PIT - SCENARIO1

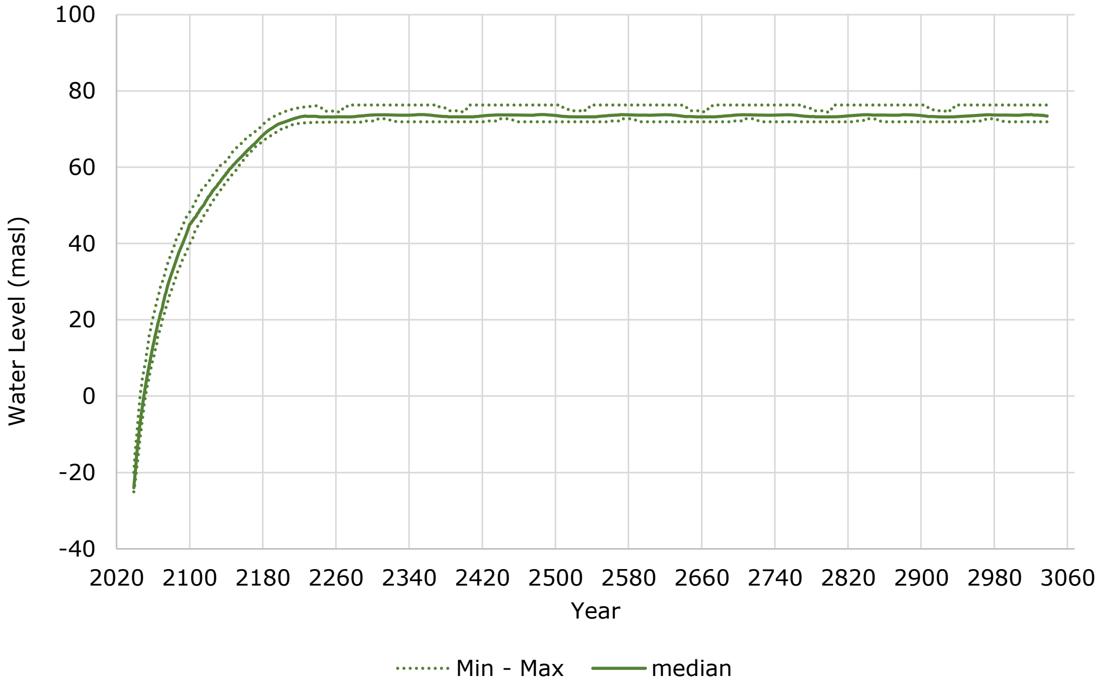

FIGURE C 1.2: PREDICTED WATER LEVEL FOR PIT 2 - SCENARIO1

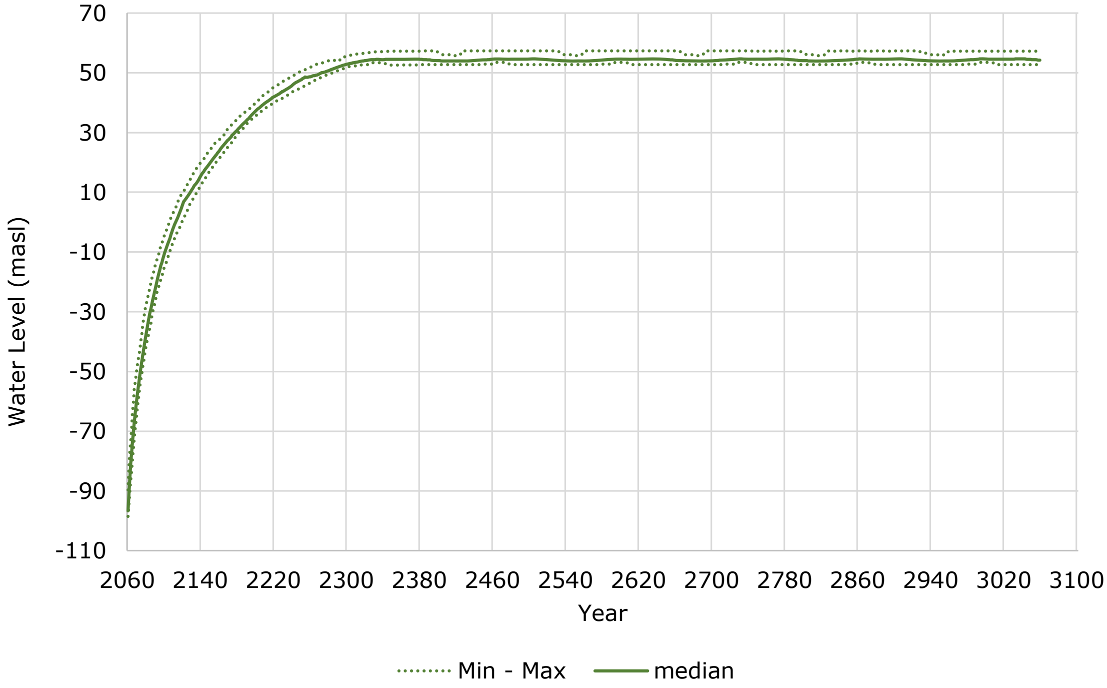

FIGURE C 1.3: PREDICTED WATER LEVEL FOR PIT 3-12 - SCENARIO1

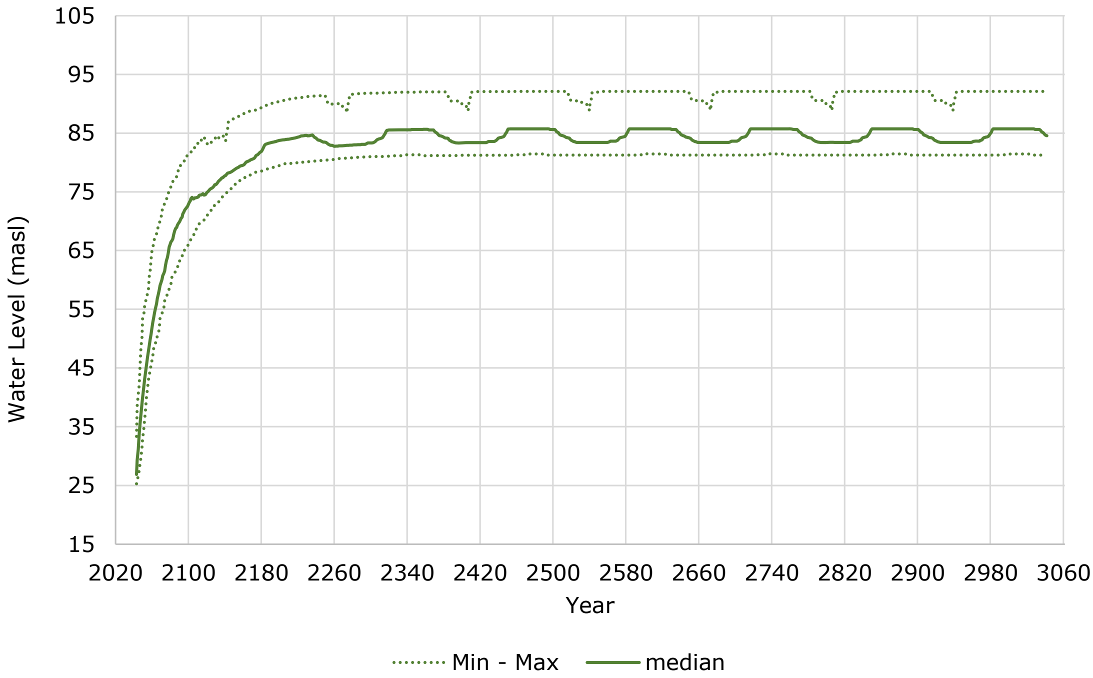

FIGURE C 1.4: PREDICTED WATER LEVEL FOR PIT 13 - SCENARIO1

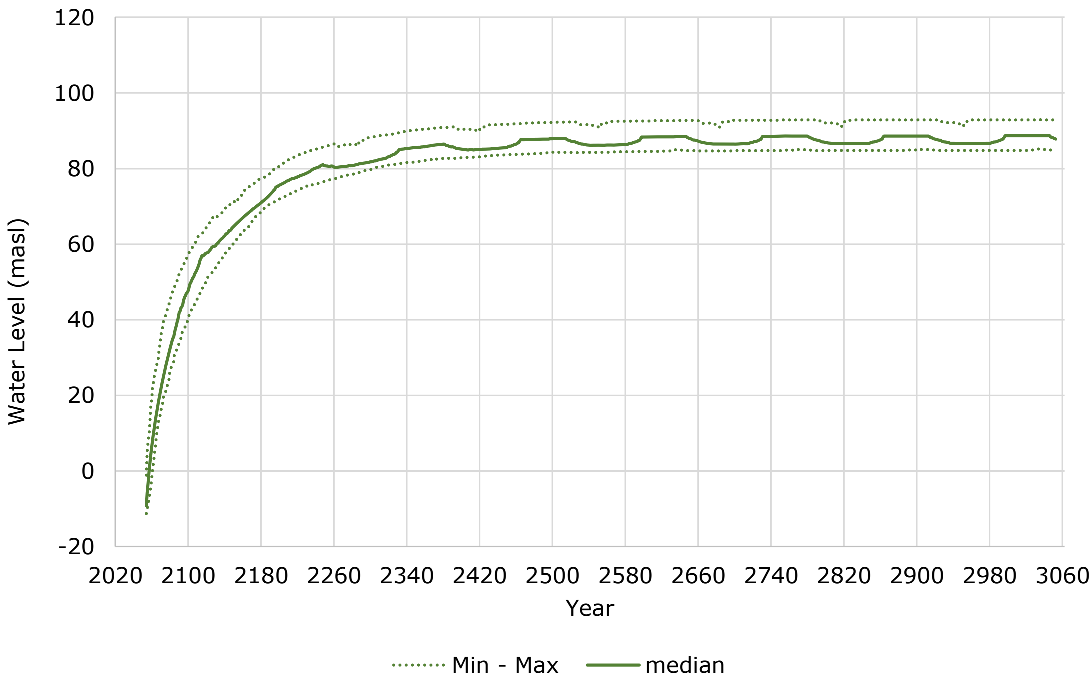

FIGURE C 1.5: PREDICTED WATER LEVEL FOR PIT 19 - SCENARIO1

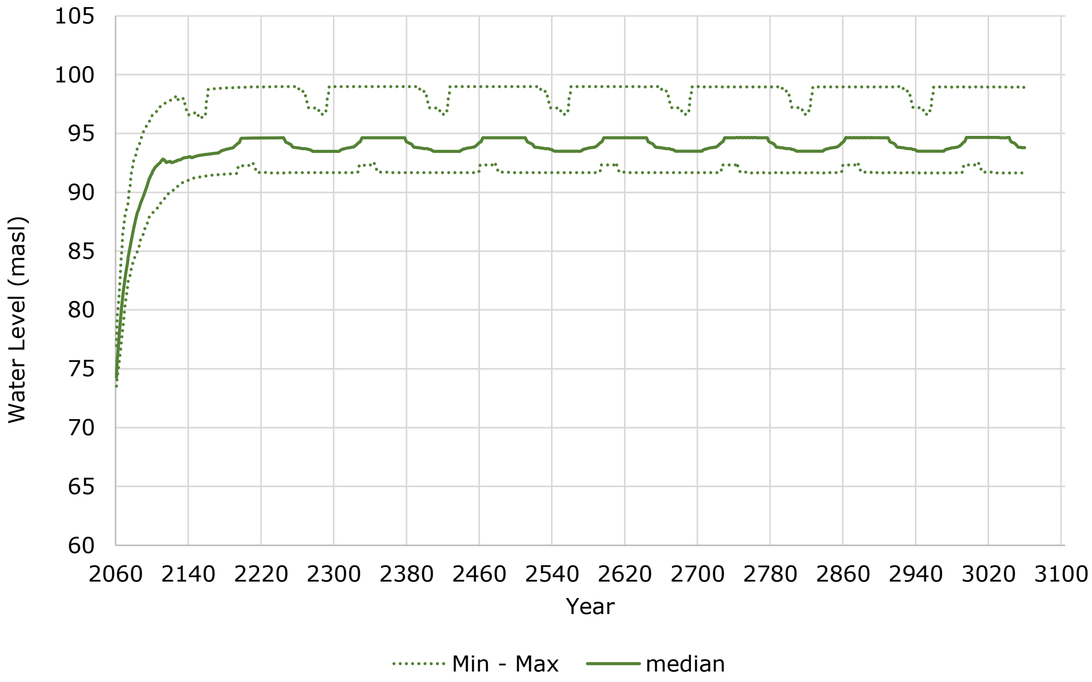

FIGURE C 1.6: PREDICTED WATER LEVEL FOR PIT 24 - SCENARIO1

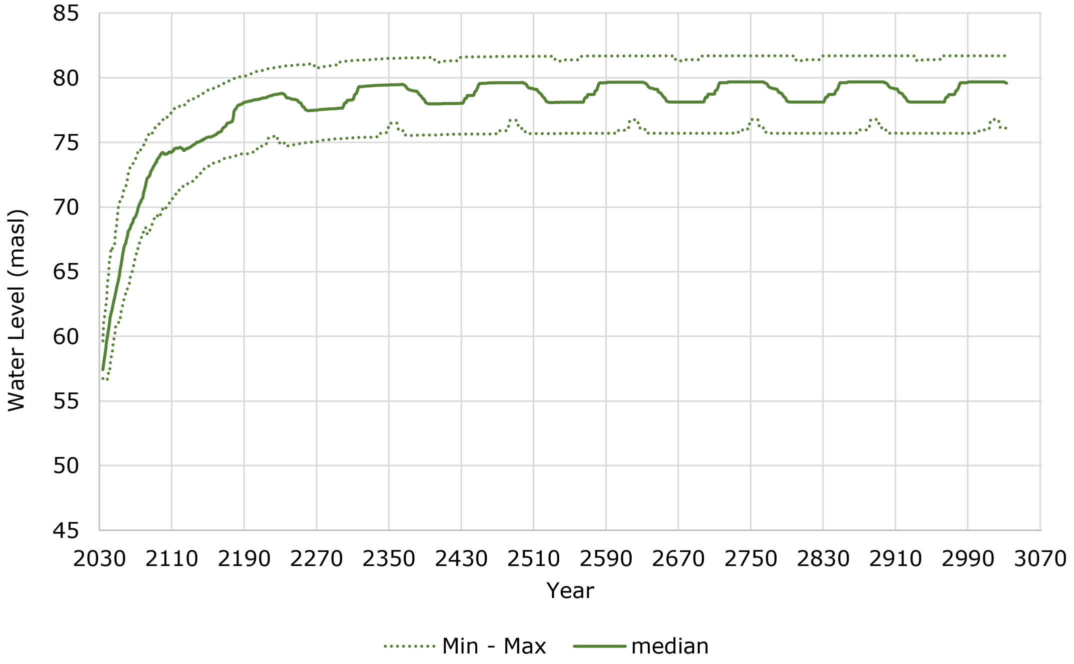

FIGURE C 1.7: PREDICTED WATER LEVEL FOR PIT 25 - SCENARIO1

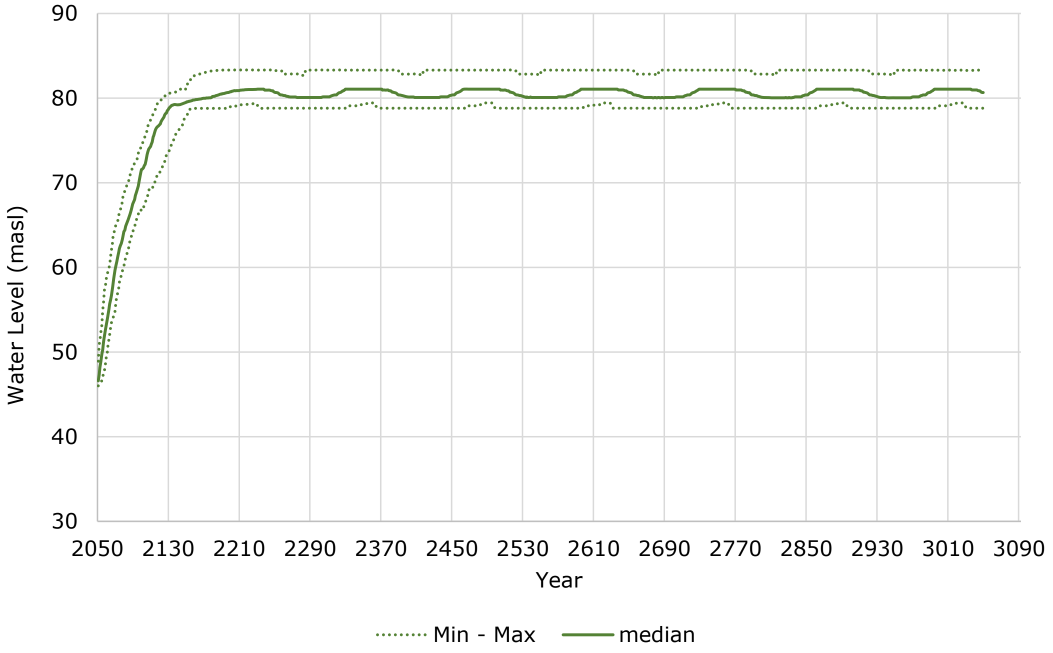

FIGURE C 1.8: PREDICTED WATER LEVEL FOR PIT 28 - SCENARIO1

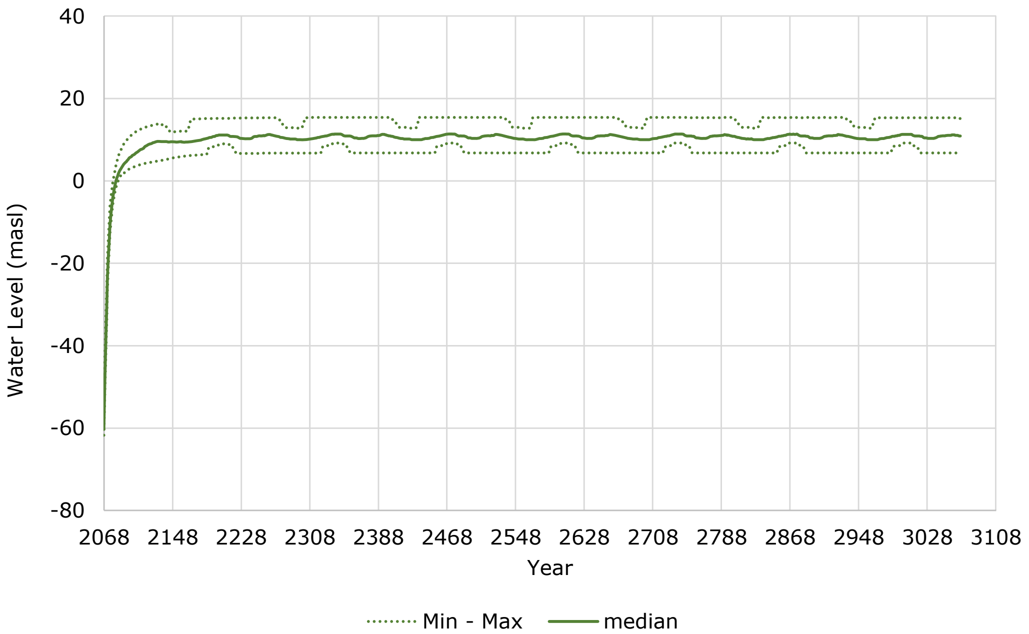

FIGURE C 2.1: PREDICTED WATER LEVEL FOR NORTH PIT - SCENARIO2

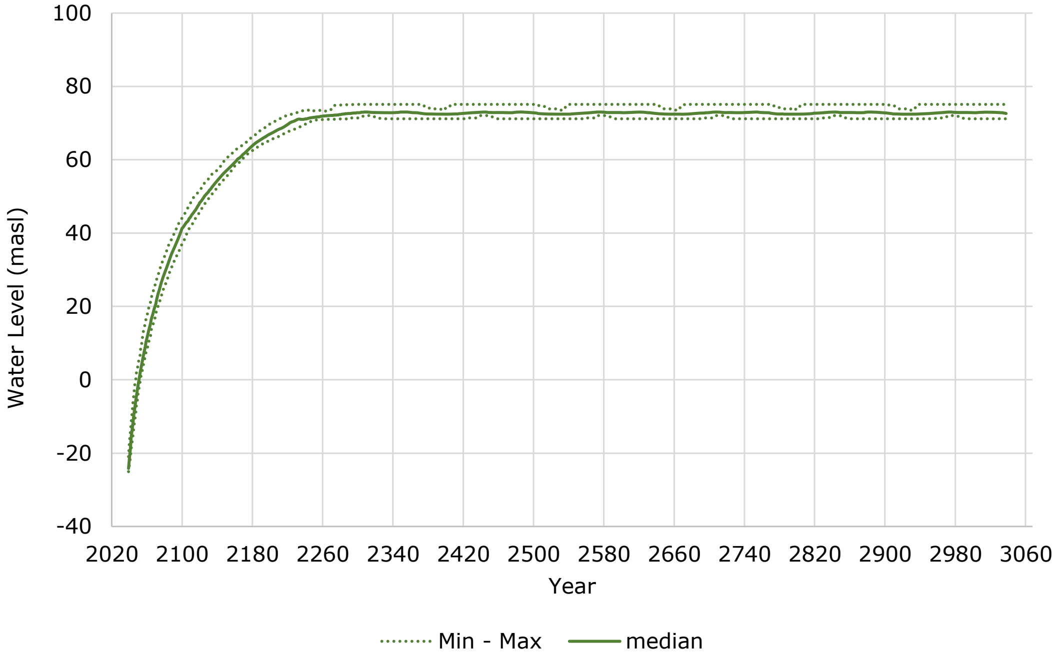

FIGURE C 2.2: PREDICTED WATER LEVEL FOR PIT 2 - SCENARIO2

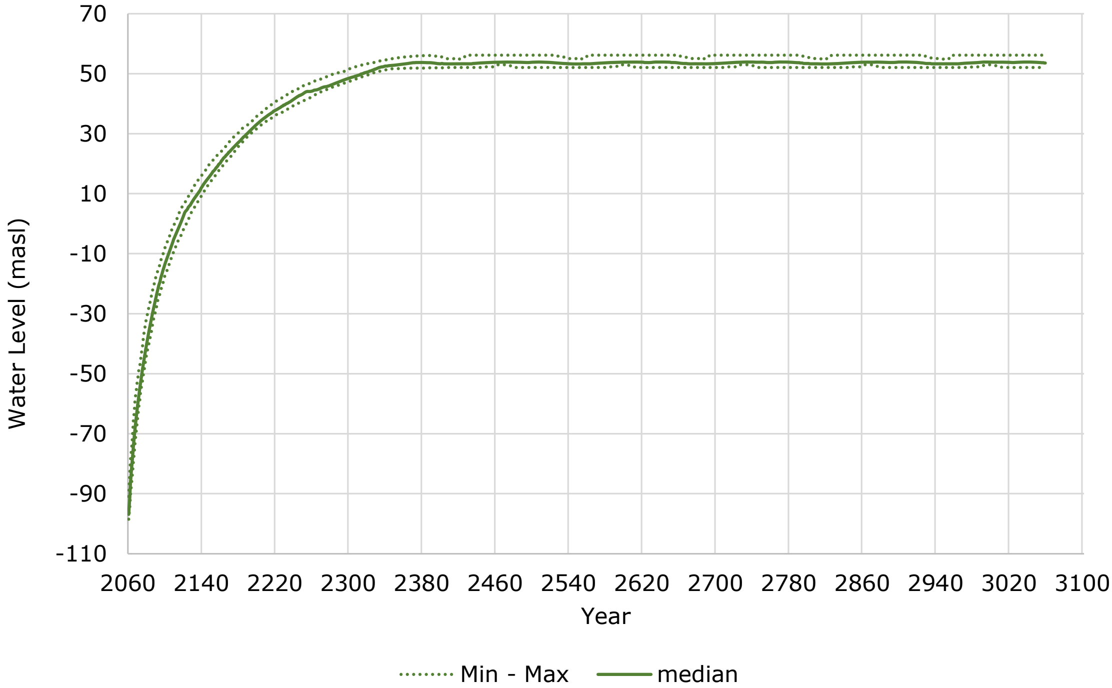

FIGURE C 2.3: PREDICTED WATER LEVEL FOR PIT 3-12 - SCENARIO2

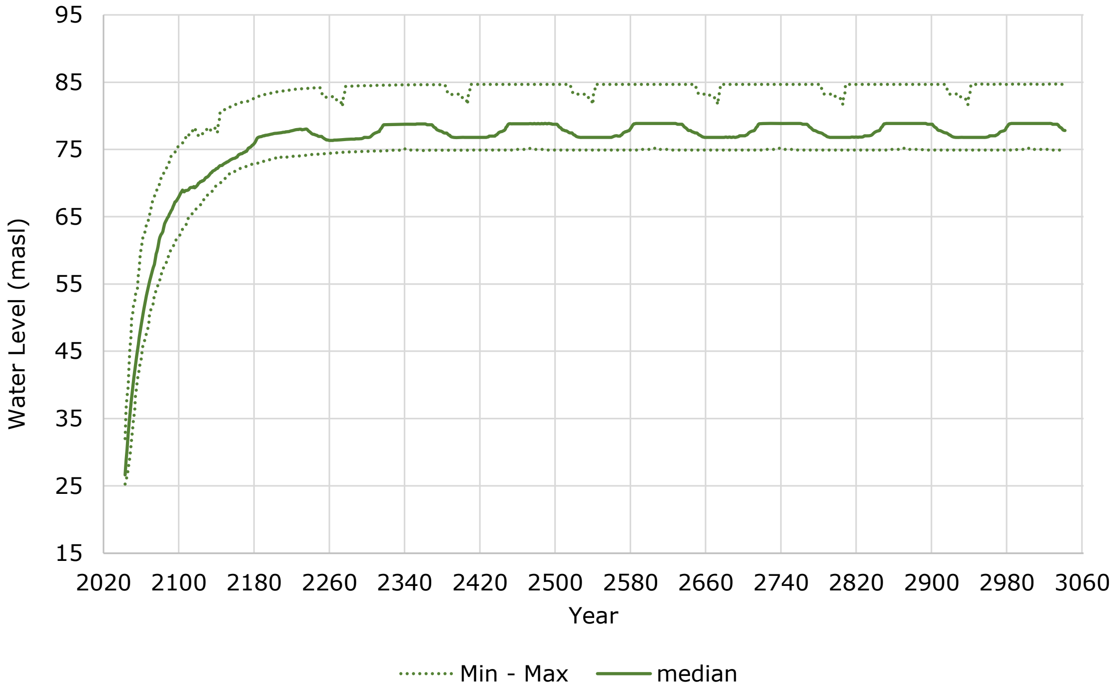

FIGURE C 2.4: PREDICTED WATER LEVEL FOR PIT 13 - SCENARIO2

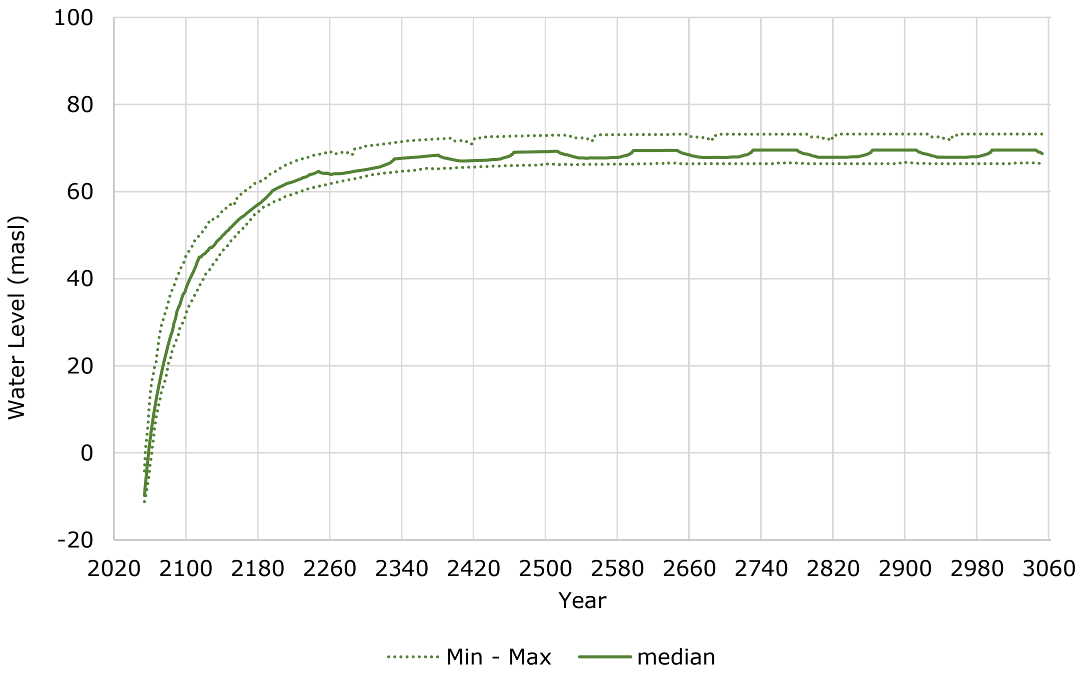

FIGURE C 2.5: PREDICTED WATER LEVEL FOR PIT 19 - SCENARIO2

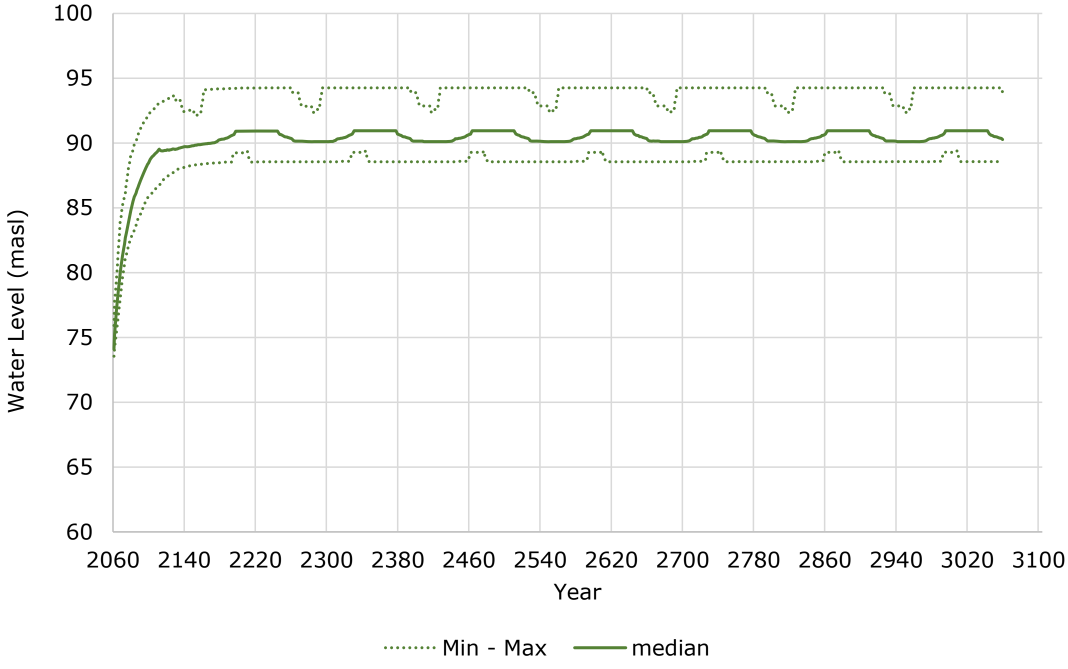

FIGURE C 2.6: PREDICTED WATER LEVEL FOR PIT 24 - SCENARIO2

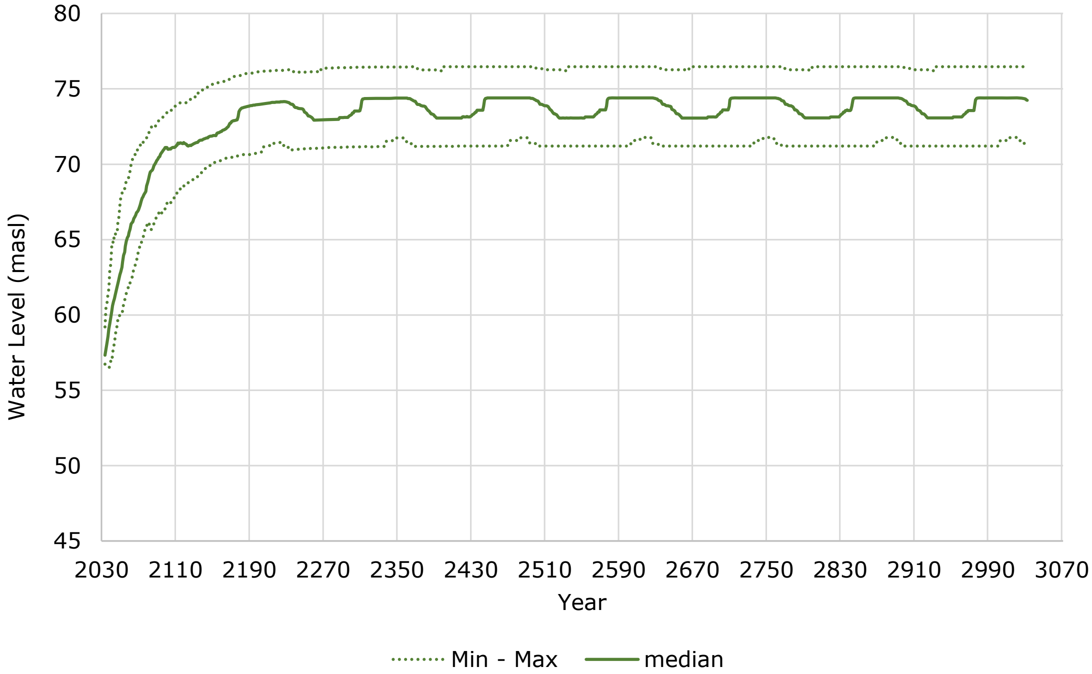

FIGURE C 2.7: PREDICTED WATER LEVEL FOR PIT 25 - SCENARIO2

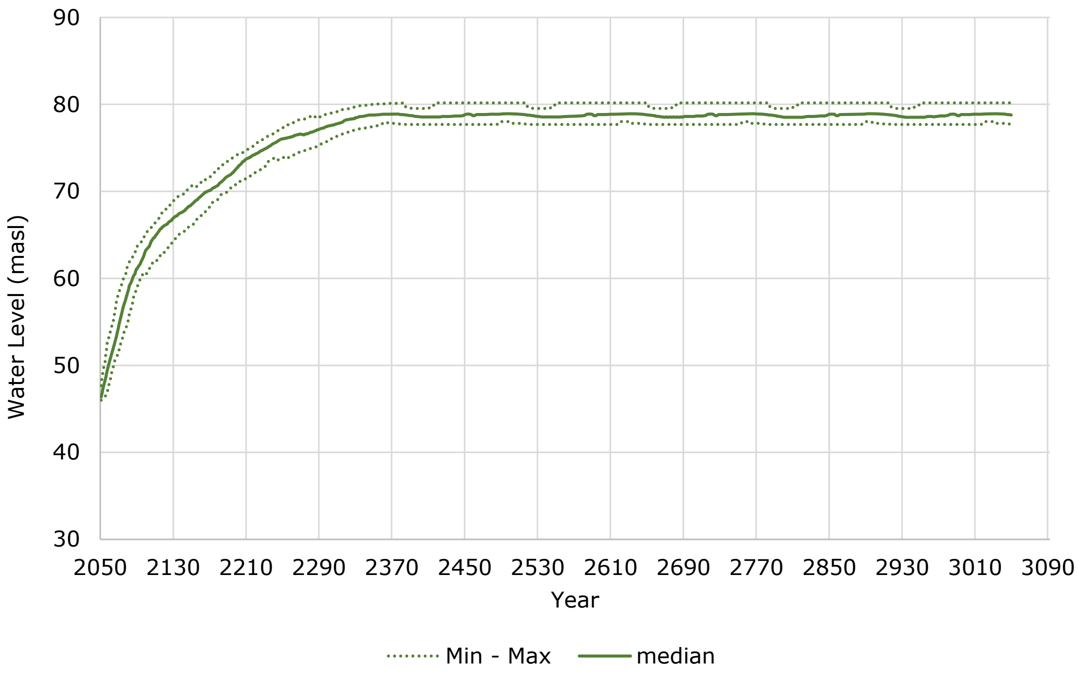

FIGURE C 2.8: PREDICTED WATER LEVEL FOR PIT 28 - SCENARIO2

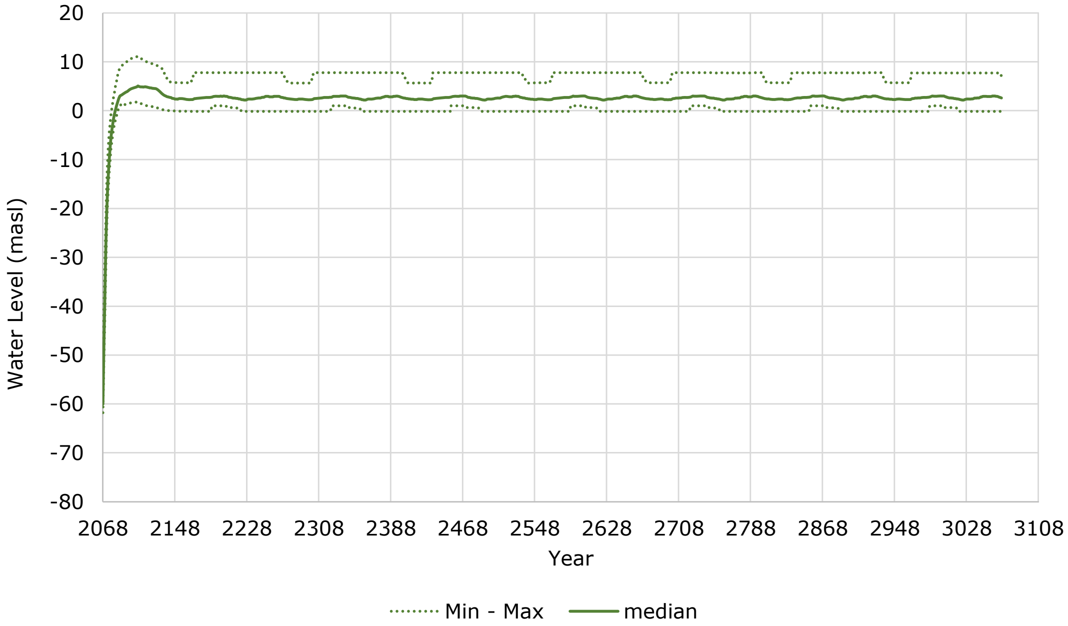

FIGURE C 3.1: PREDICTED WATER LEVEL FOR NORTH PIT - SCENARIO3

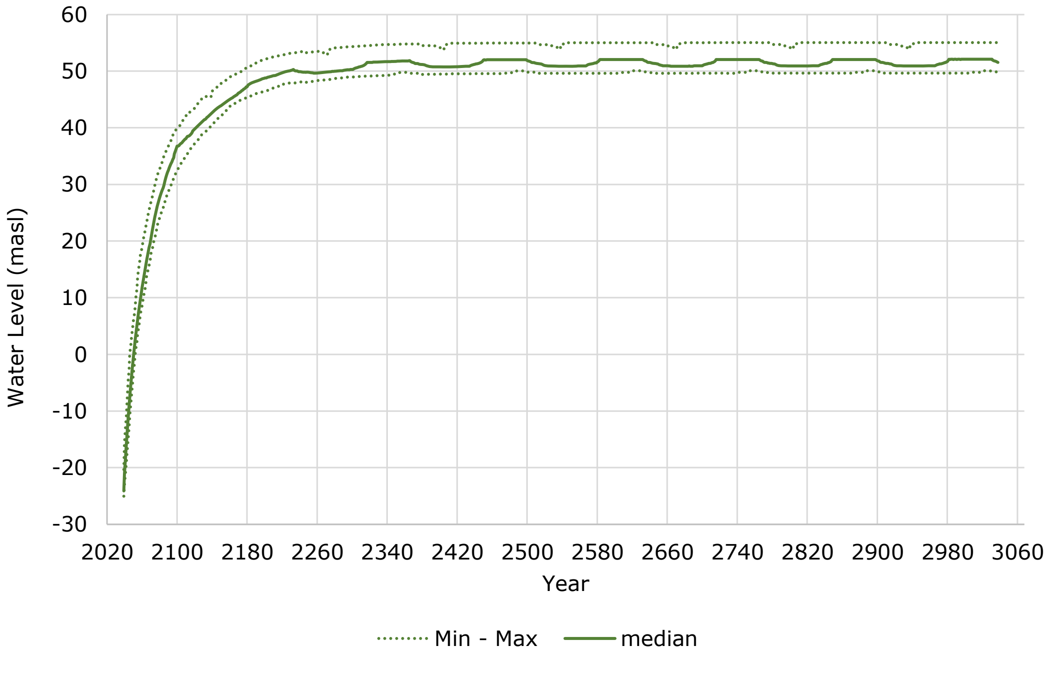

FIGURE C 3.2: PREDICTED WATER LEVEL FOR PIT 2 - SCENARIO3

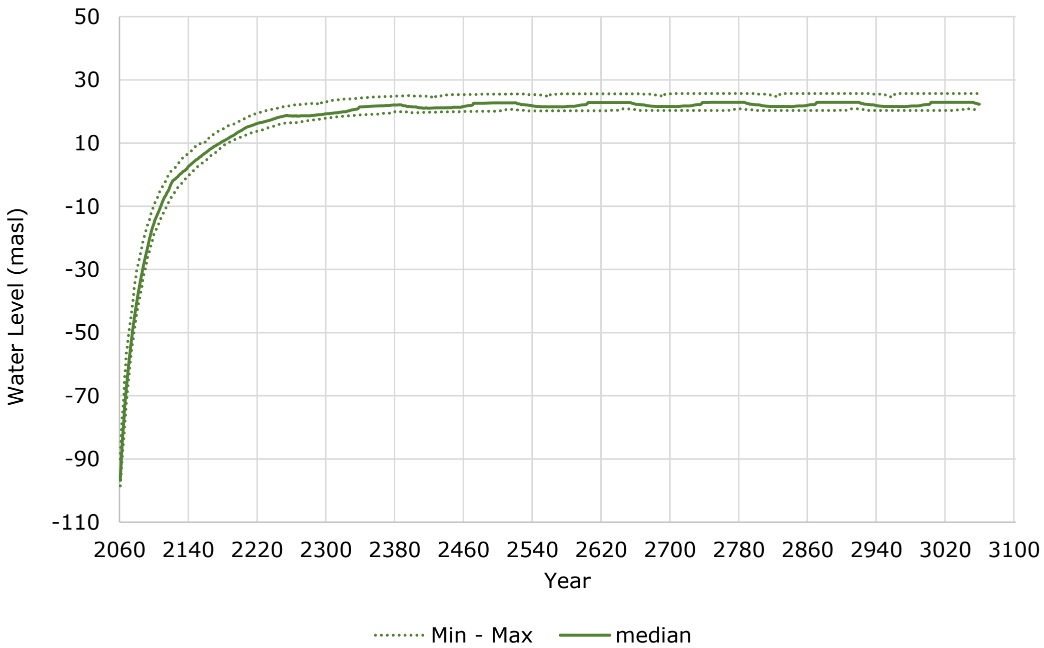

FIGURE C 3.3: PREDICTED WATER LEVEL FOR PIT 3-12 - SCENARIO3

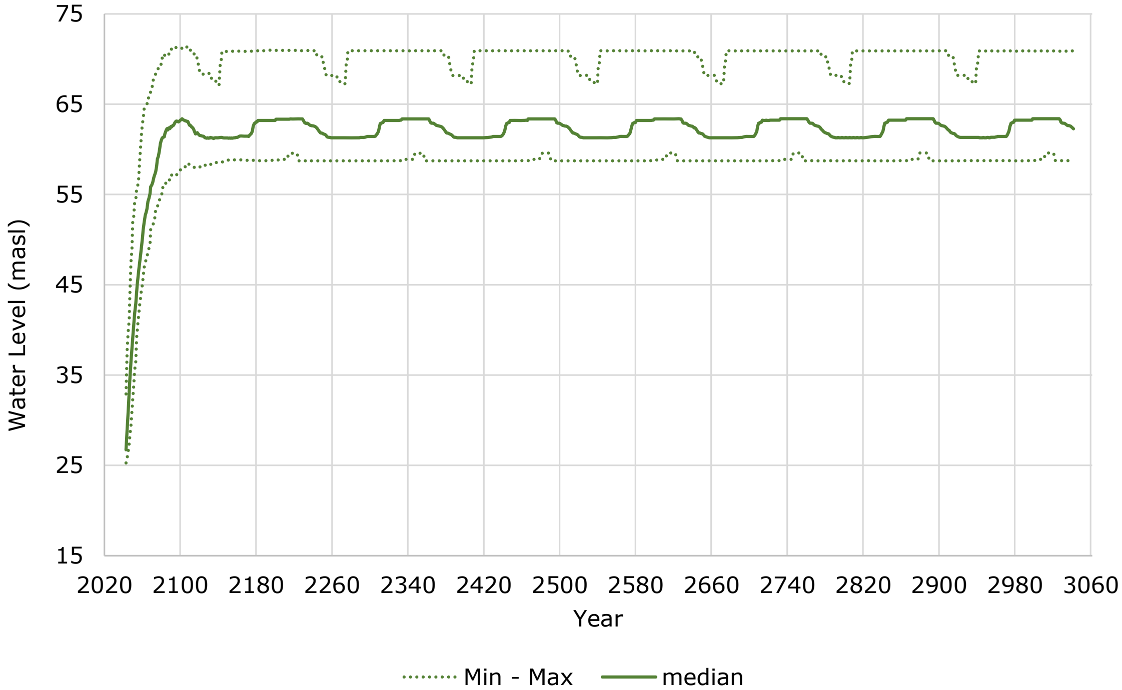

FIGURE C 3.4: PREDICTED WATER LEVEL FOR PIT 13 - SCENARIO3

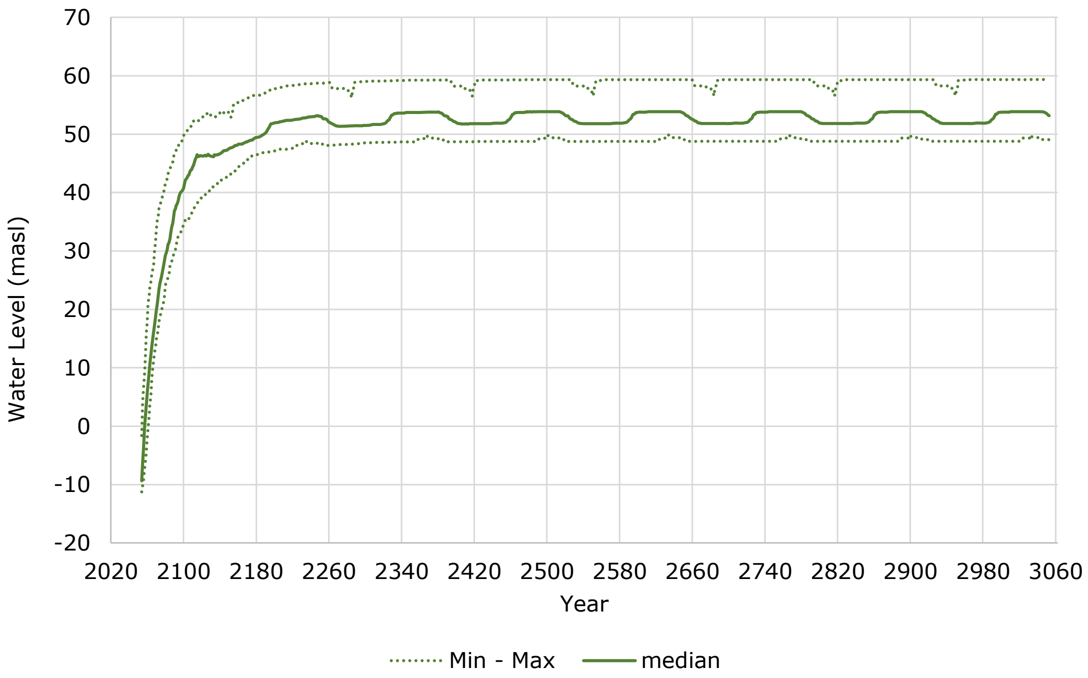

FIGURE C 3.5: PREDICTED WATER LEVEL FOR PIT 19 - SCENARIO3

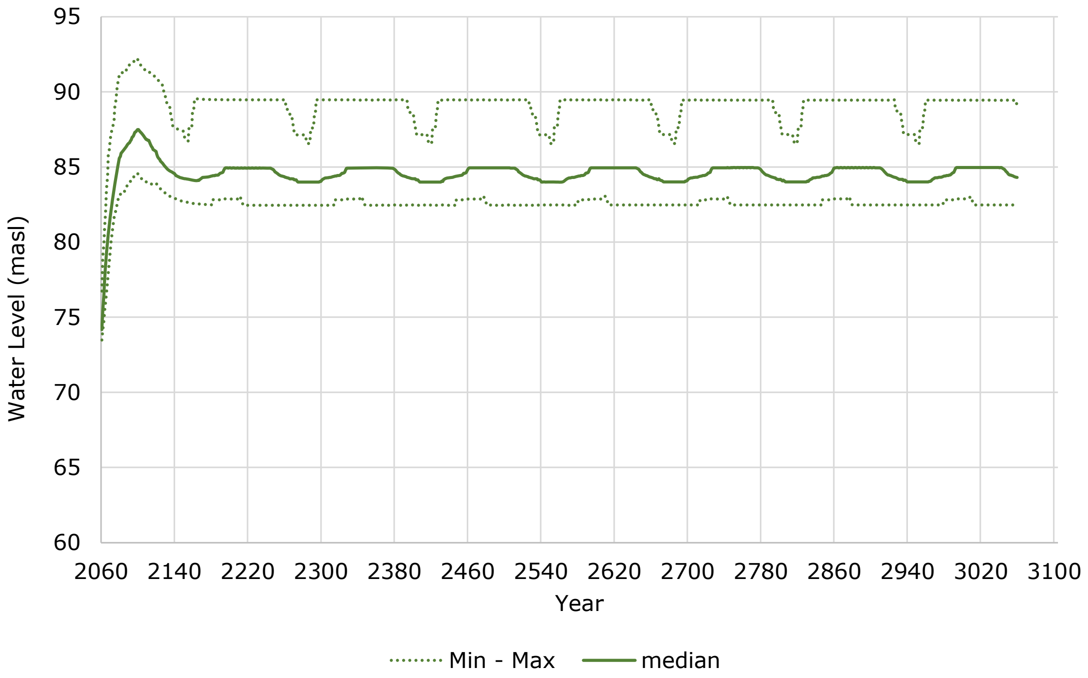

FIGURE C 3.6: PREDICTED WATER LEVEL FOR PIT 24 - SCENARIO3

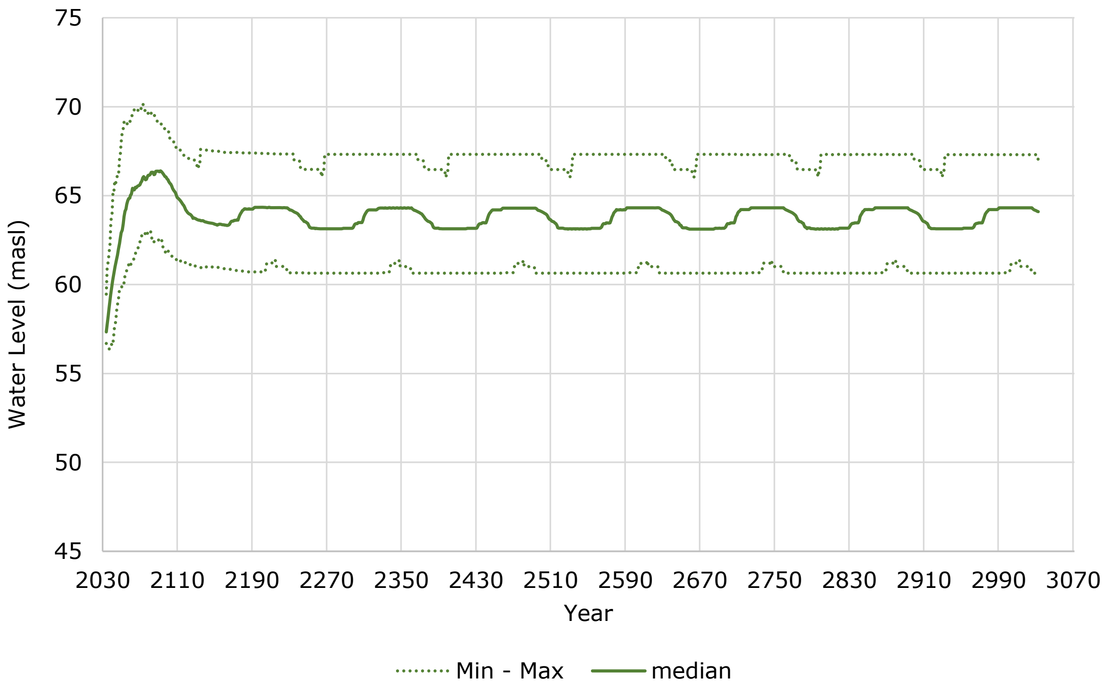

FIGURE C 3.7: PREDICTED WATER LEVEL FOR PIT 25 - SCENARIO3

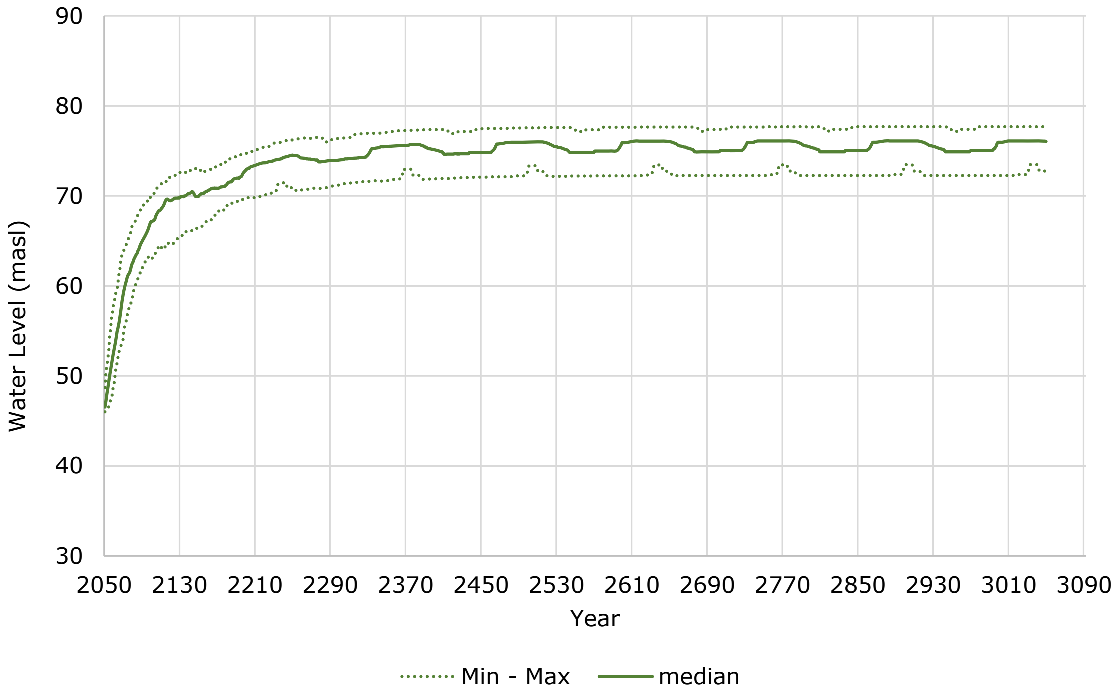

FIGURE C 3.8: PREDICTED WATER LEVEL FOR PIT 28 - SCENARIO3

ERM HAS OVER 160 OFFICES ACROSS THE FOLLOWING COUNTRIES AND TERRITORIES WORLDWIDE

Argentina
Australia
Belgium
Brazil
Canada
China
Colombia
France
Germany
Ghana
Guyana
Hong Kong
India
Indonesia
Ireland
Italy
Japan
Kazakhstan
Kenya
Malaysia
Mexico
Mozambique

The Netherlands
New Zealand
Peru
Poland
Portugal
Romania
Senegal
Singapore
South Africa
South Korea
Spain
Switzerland
Taiwan
Tanzania
Thailand
UAE
UK
US
Vietnam

ERM's Melbourne
L8, 501 Swanston St
Melbourne, VIC 3000

T: 03 9696 8011

www.erm.com